Doc. XV-293-70

Research on

THE FATIGUE BEHAVIOR OF TUBULAR CONNECTIONS

by

A. A. Toprac

and

B. G. Louis

This work has been carried out with funds
furnished by the Naval Facilities
Engineering Command, U. S.
Department of the Navy,
Washington, D. C.

May, 1970

Structures Fatigue Research Laboratory
Department of Civil Engineering
The University of Texas
Austin, Texas

S. F. R. L. Tech. Rpt. P550-13

Table of Contents

ACKNOWLEDGMENTS

The research reported herein was sponsored by the Naval Facilities Engineering Command, U. S. Department of the Navy. The investigation was carried out at the Structures Fatigue Research Laboratory of the University of Texas, Dr. A. A. Toprac, Director.

The authors are deeply indebted to Dr. Arsham Amirikian, Chief Engineering Advisor, Naval Facilities Engineering Command, Washington, D. C., for his constant support and guidance, and to Captain J. F. Dobson, Assistant Commander for Research and Development, Naval Facilities Engineering Command, Washington, D. C.

The research program on tubular connections is under the guidance of the Subcommittee on Welded Tubular Structures of the Welding Research Council, Mr. R. R. Graham Sr., Chairman. The authors wish to acknowledge the assistance rendered by the officers of the Welding Research Council, Mr. K. H. Koopman, Director and C. F. Larson, Secretary.

The assistance of the staff of Structures Fatigue Research Laboratory during the various phases of the project is acknowledged. Appreciation and special thanks are also extended to Mrs. Alice Lo for drawing the final figures and to Mrs. Pat Harris for typing the manuscript.

Abstract

This investigation presents the results of an experimental study on the fatigue strength of tubular connections. The specimens tested were T- and K-joints. All specimens had the same chord and brace which were 8 5/8" O.D x 3/16 and 3 3/4" O.D x 3/16" respectively.

Thirteen T- and eighteen K-joints were tested in this program. However in the analysis of the results previous test programs carried out at the University of Texas were also considered. These previous programs include fourteen T-joints of the same geometry. To investigate whether models can be used to make fatigue studies the above mentioned results were compared to those obtained from a fatigue study of 94 T-joints of 2¼" chord.

The results are presented in the form of S-N curves for T- and K-joints with best fit curves based on regression analysis. Further 90% survival curves are presented for both crack initiation and final failure. The study indicates that small size specimens might be feasible to study.

The results of this investigation are compared to research carried on in Japan. The correlation of the results proved to be satisfactory. Conclusions are drawn based on all these studies.

List of Figures

CHAPTER 1

INTRODUCTION

1.1 General

Recent technological developments in the fabrication of steel tubes have increased their utilization in both onshore and offshore structures. Tubes of circular cross section are excellent in resisting axial compression and torsion. Although the bending strength of a circular tube is considerably less when compared to a rolled section, it has the same strength about all axes due to symmetry. These properties permit circular tubes to carry eccentric loads more efficiently than I-shapes around their minor axis[1]*.

The limited structural use of tubes in the past was due to the relatively high cost of tubes, the lack of wide selection of sections, and the absence of established construction specifications for tubular structures. Due to recent developments tubes are now used extensively in many structures, especially in offshore drilling platforms since they develop less wind and wave forces than other shapes[2][3]. Failure of some offshore structures in recent years necessitated extensive experimental and theoretical studies to aid the design of such structures for static and fatigue loads.

---

*References are listed on page 51

shells under localized loadings. Various methods have been developed using membrane or bending theory of shells. However, these methods are applicable only to unstiffened joints and some can be used only for T-joints with restricted configurations. A review of these methods can be found in previous publications[3,4,5]. All these methods involve differential equations which make them tedious and complicated for use in the design of tubular structures. Computer programs for the analysis of unstiffened T, Y, K, and three-dimensional joints are available to compute stress distributions in some joints[6]. These methods determine the stress distribution in the elastic range only. In tubular connections the stress concentration factor, the ratio of maximum stress in the chord to the average stress in the brace, is as high as 30 in certain types of joints. Therefore, the material in the vicinity of a joint would yield under a small load, while the stress at the points away from the weld is well below the yield stress of the material. The yielding of the metal at the stress concentration points, commonly referred to as "hot spots", during the early stages of loading has no significant effect on the ultimate strength of a joint under static loading. This is due to stress redistribution at the joint. However, the yielding in the vicinity of a joint has a great effect on the fatigue strength of tubular connections.

Fracture mechanics could be used to reasonably predict crack growth; however, it cannot be applied directly to the problem of tubular joints with complex geometric configuration. Energy methods are also used to predict the fatigue limit of some simple coupons when the stress in the material is above the yield stress[7]. Again these could not be easily

points were found prior to reaching the ultimate load, especially in specimens with small β ratios. Each of these specimens had a reserve strength (the ratio of final failure load to first yield load) of twice as much as the joints with larger β ratios. Test results were used to determine equations and nomographs for the stresses around the welded T-joint[3]. In general, the critical stress in Y and K-joints was found to be at the hot point, but it had a smaller magnitude than in the T-joints[3].

The influence of joint eccentricity in K-joints was investigated[9]. It was found that joints with overlapping braces can sustain higher stresses than the other two cases of intersecting and extending braces due to the direct transfer of load between the braces.

Several types of stiffeners (gusset plates, rings, etc.) were used in the tests carried out at the University of California at Berkeley. Stress transfer between the braces and the chord, location of stress concentration, and the maximum stresses were recorded[10].

Other types of tubular connections such as cross-joints, T-joints with tubular beams and spherical joints were investigated in the U.S.A., Japan, Britain, Germany, and other countries. A summary of the investigations in the U.S.A. can be found in Reference 4.

1.5 Review of Experimental Investigations - Fatigue Tests

Fatigue tests on T-joints, consisting of two groups of specimens, were carried out at The University of Texas since 1967. In the first group there were 94 small-size T-joint specimens with 2 1/4 inch chord and five different β -ratios. They were tested under four different stress ratios (the ratio of minimum stress to maximum stress) of R = 1.0,

intersecting braces tested in this program.

1.6 Objective

The present study is part of a four-phase program initiated at The University of Texas at Austin in the Spring of 1963 under the general direction of the Welding Research Council. The four phases are:

I. Static tests of welded T-joints.

II. Static tests on T, Y, and K-joints with all members in the same plane.

III. Static tests on three-dimensional joints and fatigue tests on T-joints.

IV. Fatigue tests on K-joints.

All phases included both experimental and theoretical work. References 1, 2, 3, 8, and 16 were based on the test results of phases I, II, and the first part of phase III.

Investigations on the behavior of tubular joints under fatigue were initiated with the simple case of a T-joint as in the case of static tests. It was felt that as soon as a reliable S-N curve was established for T-joints, the more complex joints could be obtained with relative ease.

The test results of thirteen T-joint specimens reported herein comprise the last part of phase III. The primary objectives of these tests were:

a. To study the behavior of T-joints under fatigue loading, and to establish a reasonable S-N curve for crack initiation covering a range of fatigue life from one thousand cycles to more than two million cycles. Further, to make correlation

c. To perform static tests to find the locations of stress concentration points and to measure the critical stresses at these points. Also to study the stiffening effect of the inclined brace on the joint behavior.

d. To study the effect of the sign of the applied loads (axial tension or axial compression) on fatigue behavior. This aspect was previously found to have no effect for load within the elastic range.

e. To perform ultimate tests on each type of K-joints in order to observe modes of failure and to see if the joint can reach its full capacity determined by the tensile strength of one of the braces.

The geometrical parameters of series B were identical for all nine specimens except for the eccentricities. The eccentricity is defined as the distance from the point of intersection of the axes of the two braces to the horizontal axis of the chord. Positive, negative, or zero eccentricities are formed when the axes of the two braces meet below, above, or at the axis of the chord.

Series B specimens were grouped as follows:

a. Three specimens with a positive eccentricity of 2 in. (K-1, K-2, and K-3).

b. Three specimens with zero eccentricity (K-4, K-5, and K-6).

c. Three specimens with a negative eccentricity of 2 in. (K-7, K-8, and K-9).

One specimen from each group in series B is shown in Fig. 1.1. Dimensions, details, and geometrical parameters of the K-joints tested are given in Fig. 2.2. The geometrical parameters were about the same as those for the T-joint specimens in series A with a slightly smaller β ratio.

All nine specimens in series C were of the same material and had the same geometry except for eccentricities. As in series B these nine specimens were group as follows:

a. Three K-joint specimens with a positive eccentricity of 2 in. (K-10, K-11, and K-12).

b. Three K-joint specimens with zero eccentricity (K-13, K-14, and K-15).

c. Three K-joint specimens with a negative eccentricity of 2 in. (K-16, K-17, and K-18).

these cut sections. The hardness of the chord, brace, and weld materials were measured in knoops by using the Kentron Micro-Hardness Tester with a load of 500 grams applied to the etching diamond. The hardness of the chord and weld materials were approximately the same in all specimens and about 214 and 296 knoops respectively. The brace materials varied from series to series and their hardnesses were found to be on the average 335 knoops in series A, 167 knoops in series B, and 316 knoops in series C.

It was observed that the hardness of the chord materials was less (around 180 knoops) right next to the weld possibly due to the heating introduced by the welding process.

2.3 Materials

Since three series of specimens were manufactured by three different fabricators, the material properties varied from one series to another. However, all the specimens were fabricated from Grade B, Spec. API-5L, seamless line pipe corresponding to ASTM Specification A53-63T, Grade B Low Carbon Steel. Mill reports were supplied by the manufacturers.

Tensile coupons were made either from extra pipe lengths furnished by the fabricators or from the specimens after the completion of tests. These coupons were machined to the exact dimensions recommended by the ASTM Specifications for structural steel tubes, and were tested under a static tensile load in order to determine the stress-strain characteristics of the steel. Three coupons were tested for each of the six heats, and average values were obtained for modulus of elasticity, yield strength, ultimate strength, and percent elongation. Table 2.1 gives the summary of mechanical and chemical properties of steels used while Fig. 2.5 shows

Special hydraulic rams of 26.6 and 80 kips capacity were used to apply both static and fatigue loads in conjunction with a pulsator type testing machine. The fatigue load was applied at about 200 cycles per minute.

A larger hydraulic ram of 200 kip capacity with 2 1/8 in. center hole, driven by a two horsepower electric motor, was used to apply the load in the ultimate tests for series B and C. The ram was positioned inboard for compression loading which was applied through another load bar similar to the one described above and placed in a vertical position at the center of the frame. The same ram was positioned outboard for tensile loading. A load cell was used to double check the applied load as determined by a pressure gage connected to the pumping unit.

2.5 Instrumentation and Calibration

The specimens in series A were instrumented with two rosettes of 1/8 in. gage length at the hot points (S_o as shown in Appendix A). No other rosettes were placed on the chord since information about the stress distribution and stress concentration points was already available from previous investigations[3]. The two rosettes were placed as near to the toe of the weld (about 1/4 in.) as practically possible to obtain stress intensity at this critical point. Four uniaxial gages were places symmetrically in opposite sides of the brace 15 inches below the load connector plates to allow a check on the intensity of the applied load. The supports were adjusted to achieve symmetry in the application of load when the observed differences in strains were more than 4%. Figure B-1 in Appendix B shows the gage locations and details for specimens in series A.

the gage factor of the rosettes was handled by a FORTRAN computer program written to compute principal stresses.

A shake down of the set up was performed prior to testing of each specimen. Although all the possible adjustments were made, in some specimens the load was eccentric in the brace due to fabrication errors. These eccentricities were taken into account in the computer program mentioned previously for elastic stress analysis and stress concentration factors (stress in chord/stress in brace).

At the completion of an elastic test all gages around the weld were removed and the area was cleaned again with acetone. Then the specimens were whitewashed to facilitate the detection of crack initiation and propagation. Specimens tested to destruction were also cleaned and whitewashed for the detection of yield lines.

Acetone was used in monitoring crack initiation. Acetone penetrates through the faint crack, and after the surrounding surface dries out it starts bubbling out of the crack under the action of pulsating loads. This can be seen by the aid of reflected light coming from a high intensity lamp.

2.6 Test Procedure

A fatigue test was considered completed either after failure of the specimen or after two million cycles. The latter case was considered as a run-out. The run-out specimens were either subjected to a cumulative fatigue test or tested statically to destruction. Since fatigue failures under low stress ranges did not alter the configuration of the specimen, some connections with a very small crack were rewelded with a full penetration

eliminate the effect of varying P_{min}. When the 80 kips hydraulic ram was used in testing series C specimens, the lower load was increased slightly to suit the operating limits of the machine in fatigue.

The cyclic loads were applied at a comparatively low frequency of 180-200 cpm for specimens subjected to high stress ranges, whereas a frequency of 200-250 cpm were applied to specimens tested under low stress ranges. Specimens subjected to low stress range were checked for crack initiation at intervals of maximum eight hours. The inspection period for specimens tested under high stress range was frequent and in some cases continuous.

After a crack initiated, its propagation was monitored by observing its length and the corresponding number of cycles. When the cracks propagated to such an extent that failure was inevitable, the specimen was watched more carefully to avoid a sudden and violent failure. At this stage, the test was either stopped or continued until one or both braces were separated from the chord.

(c) Ultimate tests

The purpose of the ultimate tests was to determine the carrying capacity of the specimens and to observe their modes of failure.

The procedure followed was simple. The specimens were cleaned and coated with fresh whitewash to facilitate the observation of yield lines near the welds and the detection of crack initiation. The load was applied in increments. The controlling gages around the braces were monitored in the same manner as in the elastic test. The outside diameter of the chord was measured near the joint both in vertical and horizontal directions at

CHAPTER 3

TEST RESULTS OF T-JOINTS

3.1 Elastic Tests

As mentioned in Section 1.6, the objective of elastic tests was to determine the critical stresses in the vicinity of the joint and to compare them with available data from previous investigations. To accomplish this objective, measured elastic strains were converted to stresses and these in turn were compared with stresses obtained from nomographs presented in Reference 3.

Previous experimental test results have established that a steep stress gradient exists at the joint. Localized stresses are highest at the weld toe but they dampen out rapidly[3]. The stress at X_o in the X direction, σ_{xx}, (Fig. A.1), becomes essentially equal to M/S within a distance from the weld equal to the chord radius. The stress at S_o in the S direction, σ_{ss}, proved to be the critical stress in T-joints. For this reason a rosette was placed on each side of the T-joint at S_o to determine the maximum principal stress.

Table 3.1 gives the geometrical and material properties of fourteen T-joints tested previously[12] and the thirteen T-joints of this program. The load was applied as shown in Fig. 3.1, and the maximum principal stress was plotted against the measured stress in the brace for several T-joint specimens. The increase of stress at S_o was linear up to the yielding of the material as shown in Fig. 3.2.

fourteen T-joints tested in a previous program[12]. The number of cycles to the first crack and its location, the number of cycles to other cracks if any initiated, the rate of crack propagation, and the number of cycles to failure were observed.

The fatigue cracks in all the T-joints initiated at the point of stress concentration S_o. Both the calculated and measured stress concentration factor at S_o gave an average value of about 23. Since the lowest maximum stress in the brace was 2.38 ksi (T-4, 5, and 6) the actual stress at S_o was always above the yield point in all the T-joint specimens tested.

Most of the specimens cracked on one side only even though there were two points of stress concentration 180^o apart. Since the two pins supporting the chord were in the plane of the specimens, the crack formed on one side of the joint penetrated through the chord wall and propagated further inducing eccentricity in the applied force which caused the chord to rotate towards the cracked side. This rotation was instrumental in inhibiting crack initiation in the opposite side. Figures 3.4, 3.5, and 3.6 depict the failure of T-joint specimens which exhibited this mode of crack initiation and propagation. In these specimens, after the crack reached the crown, final failure occurred when the brace pulled off completely.

A second failure mode for T-joints depicted in Figs. 3.7, 3.8, and 3.9 occurs when two cracks formed in the chord either simultaneously or within a few thousand cycles from each other. The cracks propagated around the joint almost symmetrically until they were about one inch from the crown, X_o, at which time the chord wall was torn and the brace was

The ratio of number of cycles to failure, to number of cycles to crack initiation, R_f, varied from a minimum of 1.3 to a maximum of 5.2 with an average of $\bar{R}_f = 2.13$. The sample standard deviation was $s = 0.57$. Using a 90% confidence limit and a normal distribution curve[15] $R_f = 1.4$ was obtained indicating that 90% of the joints tested under fatigue, with the same pattern of loading, will have a failure to first crack ratio R_f larger than 1.4.

3.5 Regression Analysis and the S-N Curves for T-joints

The problem of analyzing and interpreting certain observations is frequently encountered when dealing with experimental data. The aim of such analyses is to determine the form of relationship among variables. However, no exact form of this relationship can be obtained when the phenomenon involves a large number of parameters. Usually the number of independent variables is reduced omitting parameters which have small influence on the final value of the dependent variable.

Such a procedure has been followed in the analysis of the fatigue test data of this investigation in which stress range, minimum stress, frequency of load application, yield point, ultimate strength, percent elongation of the material, temperature during testing, welding procedure, residual stresses, weld contour, geometry of weld, and weld defects possibly are the independent variables. However, previous studies on similar fatigue problems have indicated that stress range had the major influence on the fatigue life of structural members. In this study the effect of most variables, except that of stress range was assumed to be minimal and the welds were assumed without defects and the influence of welding

A semi-log expression was also used in an attempt to determine a more suitable curve that fits the test results with the least standard error of estimate. The regression analysis was done on the same 27 test results with the difference that S_r was used instead of Log (S_r x 10) and the equation became:

$$\text{Log } (N \times 10^{-3}) = 3.77162 - 0.56492\ S_r \qquad \text{(Eq. 3.4)}$$

This equation is easier to use and it gives a standard error of estimate of 0.3075 which is very close to that for the log-log expression. The semi-log equation is also shown in Fig. 3.11 as a straight line.

3.5.2 S-N Curve for Failure - An expression for the number of cycles for failure of T-joint specimens in terms of the stress range was derived using the same regression analysis procedure described above. The log-log equation whose standard error of estimate is 0.2206 was:

$$\text{Log } (N \times 10^{-3}) = 7.00197 - 3.35601 \text{ Log } (S_r \times 10) \qquad \text{(Eq. 3.5)}$$

This equation is shown in Fig. 3.12. The semi-log form was also used and it resulted in the following equation:

$$\text{Log } (N \times 10^{-3}) = 3.78159 - 0.49172\ S_r \qquad \text{(Eq. 3.6)}$$

Figure 3.12 represents the latter equation with a standard error of estimate of 0.2131. The standard error of estimates for the last two expressions (S-N curve for failure), indicate that there is more consistency and less dispersion among the failure data than the data for crack initiation.

As for the evaluation between the log-log and semi-log expressions, it was found that the semi-log equations represent the population better

with 85% confidence limit, and gave a similar result revealing that the number of 1.100 cycles does not belong to the S-N curve derived for crack initiation in T-joint prime specimens.

3.7 Microscopic Investigation of the Fatigue Crack

Specimen T-13 was tested under fatigue to investigate crack propagation through the chord wall. It was observed from previous tests that the fatigue crack of a joint is initiated at the toe of the weld and at the outside surface. It was also observed that the crack propagates much faster in length than in depth. Consequently, the crack propagation theories which are derived for simple notched coupons, where the crack propagated in one direction through the total thickness[17], cannot be applied for the crack discussed herein.

The main purpose for testing specimen T-11 was to confirm the previous observations and to determine the dimensions of the crack. The specimen subjected to S_r = 3 ksi in the shear area was watched until the first crack developed at N = 96,000 cycles, and the length measured only from the surface was found to be 0.9 in. The test was stopped when the crack length became 2 in. at N = 106,000 cycles and the joint was cut out of the specimen. Another cut was again made through the middle of the crack to measure crack depth as shown in Fig. 3.13. After smoothing the surface of the cross section by Emery cloth, the area around the weld section was etched by applying diluted nitric acid to the smooth surface of the joint until the weld became visible. The crack was then measured using a Kentron microscope and was found to be 2.05 inches long with 0.061 inch depth (1.55 mm) in the center. It was clearly seen under the microscope that the crack initiated

CHAPTER 4

TEST RESULTS OF K-JOINTS

4.1 Elastic Test

Since the elastic test results of welded K-joints varied significantly according to their geometry, they are discussed separately in this chapter. Previous studies indicated that specimens with inclined braces such as Y-joints, have smaller stress concentration factors than T-joints with the same geometrical parameters[3]. This decrease in stresses is due to an increase in shear area by a factor of $1/\sin\theta$, where θ is the angle between the brace and the chord axis (θ = 45 degrees in the K-joints of this program).

To provide static equilibrium, the inclined brace in all the K-joints was subject to a load of 1.414 times the load applied to the vertical brace with opposite sign. The forces in the chord and braces are shown in Fig. 4.1. The absolute value of the stresses around the joint in series B specimens, was found to be the same as in series C specimens. Since the shear area of the inclined brace is $1/\sin\theta$ times that of the vertical brace, the average shear at the joint was the same for both braces.

The K-joints with extended braces (positive eccentricity) were tested first in both series B and C so that the influence of adding an inclined brace to a T-joint could be studied more easily. The measured principal stresses at the location of the rosettes around the weld (Fig. B.2) in K.1, 2, 3, 10, 11, and 12 proved that the maximum principal stress is still

needed for equilibrium were transferred through the chord. The measured maximum principal stresses for these joints were the smallest in any of the K-joint specimens tested in this program.

The overlapping braces in the K-joint introduced a critical high principal stress in the inclined brace at its intersection point with the other brace. As in other points of stress concentration, the critical stress was at the toe of the weld, and the stress in this critical location was very sensitive to any bending moment in the plane of the joint. Rosette strain gages were placed at location (10) (Appendix B - Fig. B.4) to investigate the influence of the overlapping brace on the stresses at this point.

It was found that while S_o was still the critical point, the stresses in the chord around the joint were more uniform. Thus, cracking modes under fatigue, as discussed in the following section, were different than those observed in T-joints. Based on measured stresses in K-7, 8, and 9 in series B, and K-17 and 18 in series C specimens, the average values of stress concentration were 8.6 at S_o, 7.2 at S_o', and 5.4 at the point of intersection of the two braces. A summary of the geometrical properties of the 18 K-joints, the mechanical properties of the steel, and the loading patterns are given in Table 4.1.

4.2 Fatigue Cracks in K-joints - Series B

Since K-joints have a more complicated configuration than T-joints, crack propagation and modes of failure are different among connections with extended, intersecting, or overlapping braces. Fatigue test results are summarized in Table 4.2 for series B specimens.

gating around the joint. A second crack was also developed in both joints and the test was stopped when a small portion of the chord wall was still holding (Fig. 4.7) or when complete separatinn of the two braces from the chord took place as one piece (Fig. 4.8). No crack initiated at the overlapping portion of the two braces.

4.3 Fatigue Cracks in K-joints - Series C

The loads applied to the nine K-joint specimens in series C were a tensile load in the inclined brace equal to 1.414 times the compressive force in the vertical brace (Fig. 4.1.a). The specimens in this series had a considerably longer life than the specimens in series B. Table 4.3 gives a summary of the fatigue test results in series C specimens.

The specimens are grouped according to the type of eccentricity as follows:

a) K-joints with extended braces (K-10, 11, 12; e = + 2") were subjected to the stress ranges of 2.3, 6.85, and 9 ksi in the vertical brace respectively. K-10 and K-11 developed the first crack at the toe of the diagonal brace to chord weld near the crown as shown in Figs. 4.9, 4.10, and 4.11. The maximum principal stress at S_o was compressive and was smaller than the maximum principal tensile stress measured at the crown where the crack formed. Figure 4.11 shows specimen K-12 which had four cracks forming separately; the first one occurred near S_o and towards the inclined brace. The second crack was at the crown as in specimens K-10 and K-11. The third crack was symmetrical with respect to the first, while the fourth developed at the inclined brace, at a small distance from the crown.

brace. The cracks initiated in four different locations and propagated completely around the joint. Initiation of cracking took place at 15,650 cycles and failure at 35,260 cycles.

4.4 Fatigue Crack Propagation in K-joints

Parameter R_f, which is the ratio of the number of cycles to failure divided by the number of cycles to crack initiation, was larger for the K-joints with intersecting and overlapping braces than for T-joints. This was most probably due to the longer weld length in the K-joints. The fatigue crack propagation of sixteen K-joints is shown in Fig. 4.17 in which the length of fatigue crack is plotted as a function of the number of cycles.

The average value of R_f was equal to 2.87, but the scatter of the data (1.08 to 6.8) in these specimens resulted in a comparatively high sample standard deviation making it difficult to present a safe value for R_f in K-joints with a reasonable confidence limit.

4.5 S-N Curves for K-joints

The fatigue test results indicated that the different types in series B and C cannot be grouped in one S-N curve because of the large scatter of the test results. However, each group that consisted of three specimens with exactly the same dimensions and loading pattern gives a curve which seems to correspond to the general trend of the S-N curve previously established for the T-joint specimens.

Figure 4.18 shows the number of cycles to crack initiation in the eighteen K-joints tested in series B and C and the corresponding S-N curve for T-joint specimens. It should be noted that all points for the K-joints fall above the line for the T-joints. A dotted line is drawn through points

of that brace calculated from coupon test results was 112 kips and its strength at yield 65.5 kips.

The excessive deformation of the joint after the buckling of the chord wall, caused the tearing of either the brace under tension at the toe of the weld, or the chord wall right under the tensioned brace as shown in Figs. 4.21 and 4.22. In Table 4.4 the ultimate loads in the braces at failure are tabulated.

It can be seen clearly that the ultimate strength of a joint increases when the braces overlap. It is interesting to note that the maximum average stress developed in the inclined brace of the overlapping joint in series C was σ_{max} = 63.3 ksi which is about 88% of the yield stress in the brace material (σ_y = 72.5 ksi).

from test results. For design purposes, 90% survival curves for crack initiation and failure were obtained for the T-joint specimens using the standard error of estimate as specified for each curve and assuming a normal distribution of the universe. The survival curves shown in Fig. 5.1 below the corresponding best fit curves, indicate that 90% of any number of T-joint specimens, identical to the joints reported herein, will have a life longer than the one specified by the survival curve. Thus, the equation describing the 90% survival curve for crack initiation is:

$$\text{Log } (N \times 10^{-3}) = 3.37802 - 0.56492\ S_r \qquad \text{(Eq. 5.1)}$$

and for failure is:

$$\text{Log } (N \times 10^{-3}) = 3.50882 - 0.49172\ S_r \qquad \text{(Eq. 5.2)}$$

5.3 Comparison with Small T-joints

The fatigue test results of the small T-joints[11] tested at the University of Texas gave a large dispersion when the specimen lives were plotted against the stress range only. Table 5.1 gives a summary of the fatigue test results of 85 small T-joint specimens grouped according to τ, the ratio of the thickness of brace to the chord thickness. Figure 5.2 shows the eight-five points with the S-N curve (best fit curve) for each type of joint.

An attempt was made to explain the large scatter of test results of these specimens by introducing new variables which were observed to have a noticeable influence on the fatigue life. A regression analysis was made to correlate the fatigue life of the small T-joints to the stress range multiplied by τ and divided by the ultimate strength and the percent

ratios, namely from 1 to 0.6 and ϵ_t values of twenty-seven to fifty-four. Nevertheless, Eq. 5.4 shows that, maybe, fatigue data obtained with prototype and model T-joint specimens could be correlated when influencing variables such as τ and ϵ_t are introduced.

5.4 Comparison with T- and X-joints (Japan)

Fatigue tests on tubular joints made in Japan[18] include three types of T-joint specimens (T-joint without reinforcement, with brackets, and with gusset plate) as shown in Fig. 5.5. Only four Type I specimens without reinforcement were similar in geometry to the T-joints reported herein. However, the tension load P was applied as shown in Fig. 5.5, inducing critical stresses in the crown where the measured stress concentration factor was equal to 5.2. Since the load pattern is different, no attempt was made to correlate these results.

Seventeen X-joint specimens were also tested in fatigue[18, 19], out of which eleven specimens were without reinforcement as shown in Fig. 5.6. The testing and the load application procedure was similar to the T-joints reported earlier, except for the reaction forces in the chord which were zero in the X-joints. Fatigue test results of eleven X-joints at failure are shown in Fig. 5.7. The fitted curve was found to be parallel and below the S-N curve of Eq. 3.6.

The two lines are comparatively close and the difference can be explained by the fact that the chord in X-joints has to sustain more deformations than in T-joints. Such deformations reduce the stiffness of the chord around the joint inducing higher stresses at the hot spot. Another reason for this difference is that the test data corresponding to T-joints

5.6.1 Comparison with K-joints in Japan (I)

Eleven full-scale tubular K-joint specimens used for a crane jib were tested under fatigue in Japan[20]*. Each specimen had a total of three braces and two chords forming a truss type specimen. However, the tested joint had two extended braces welded to the chord at 45^{o} as shown in Fig. 5.8. The chord was pre-compressed and the fatigue was applied to the joints by fixing one end of the truss and loading the other laterally in the plane of the specimen.

Test results are plotted as an S-N diagram shown in Fig. 5.9. These K-joints were compared with the extended case of K-joint specimens in series C (K-10, K-11, and K-12) since both types of specimens had the critical tension stresses at S_o' (see Fig. A.1) and both had extended braces. The failure data of K-10, 11, and 12 lie below the rest of the specimens in Fig. 5.9 because the life of the joints are plotted against the stress range in the brace and not in the shear area where the critical stresses are located. The same data is plotted in Fig. 5.10 taking into account the chord thickness by multiplying the stress range by the τ ratio. From Fig. 5.10, it can be clearly seen that all points fall near one fitted line except for the specimens with τ ratio of 0.564 which fall above the rest of the joints indicating that the critical value of τ ratio is very close to 0.56 as observed in Sec. 5.5. Thus, all the specimens mentioned above cracked in

---

*The specimens were identical except for the chord thickness which was 6.6" O.D. x (0.18", 0.24", and 0.284"). The brace was 3.0" O.D. x 0.16" for all specimens resulting in a τ ratio of .89, .667, .564 respectively.

in Fig. 4.11). The other failure mode was essentially controlled by the separation of the tension brace from the chord wall due to crack propagation. The cracks were invariably found at very low cycles along the toe of the weld at the crown of the chord.

Table 5.2 gives a summary of the fatigue test results while Fig. 5.12 shows the S-N relationships of the twenty-two specimens at failure. These K-joints had the braces welded apart at about one third of an inch (measured at the crown between the toes of the weld). Therefore, it seemed logical to compare these specimens with the K-joints of series C specimens having extended and intersecting braces (K-10 through K-15). Figure 5.12 shows the S-N relationship between the K-joints mentioned above which seem to lie between the two solid lines which represent the Texas results. The large scatter of the Japanese test results is due to the difference in the welds of the joints (two welders did the welding of the joints). It should be pointed out also that the data are usually more scattered at high stress ranges (low cycle) if only because of the logarithmic scale. Further certain factors which tend to be less effective at low stress ranges become quite important at low cycles.

4. The present study together with the available test results showed that in both T- and K- joints τ ratio should be 0.56 for optimum results.
5. The design criteria to be formulated should be based on the stress in the shear area, irrespective of the type of tubular joints (T-, Y-, or K- joint).
6. Based on the available test data, S-N curves were established for T and K-joint specimens.
7. Since the fatigue study involves a considerable number of test data to obtain needed design criteria, specimens with small tubular members could be used to study the fatigue behavior of tubular joints.
8. The present study resulted in obtaining 90% survival curve for T-joints. This curve can be used in evaluating the fatigue life of T-joints.
9. The difference between the number of cycles at crack initiation and at failure varies depending on the stress range to which the specimen is subjected. This ratio shows the "fatigue reserve life", and this could be considered in formulating design criteria.
10. Joints tested under high stress ranges failed in a manner similar to a ductile failure of the joints under static loads, where local creep-like deformations in the chord wall near the compression braces increase progressively till final failure occurs. Failure of the joints under low stress ranges is due to crack propagation in the chord wall.

REFERENCES

1. Horton, S. B., and Toprac, A. A., "Investigation of Elastic Stresses in Welded Tubular Steel K-joints," Structures Fatigue Research Laboratory, Report No. P550-6, The University of Texas, Austin, January 1966.

2. Toprac, A. A., "Stresses at Intersection of Tubes: Cross- and T-joints," Journal of Petroleum Technology, May 1967, pp. 695-702.

3. Beale, L. A., and Toprac, A. A., "Analysis of Inplane T, Y, and K Welded Tubular Connections," Bulleting No. 125, Welding Research Council, New York, N. Y., October 1967.

4. Natarajan, M. and Toprac A. A., "Studies on Tubular Joints in U.S.A. Review of Research Reports," Structures Fatigue, Research Laboratory, The University of Texas, Austin, May 1969.

5. Toprac, A. A., Johnston, L. P., and Noel, J., "Welded Tubular Connections: An Investigation of Stress in T-joints," Welding Journal Research Supplement, January 1966.

6. Technology Laboratories, Inc. of Austin, Texas (Private Communication from Company and Professor A. A. Toprac).

7. Munse, W. H. and Grover, La Motte, "Fatigue of Welded Steel Structures," Welding Research Council, New York 1964.

8. Brown, R. C., and Toprac, A. A., "An Experimental Investigation of Tubular T-joints," Structures Fatigue Research Laboratory, Report No. P550-8, The University of Texas, Austin, Texas, January 1966.

9. Bouwkamp, J. G., "Behavior of Tubular Truss Joints under Static Loads," Structures and Materials Research, Report No. SESM-65-4, College of Engineering, University of California, Berkeley, July 1965.

10. Bouwkamp, J. G., "Structural Behavior of Tubular Joints with Wing-Plates," Structures and Materials Research, Report No. 67-32, College of Engineering, University of California, Berkeley, December 1967.

11. Kurobane, Y., Natarajan, M., and Toprac, A. A., "Fatigue Tests of Tubular T-joints," Structures Fatigue Research Laboratory, The University of Texas, Austin, Texas, November 1967.

TABLES AND FIGURES

Series	Section of the Specimen	Type of Report	Physical Test				Chemical Analysis			
			Elastic Modulus ksi	Yield Strength psi	Ultimate Strength psi	% Elong. in 2 inches	C	Mn	P	S
A	Chord	Mill rept		48,600	60,100	30	.24	.64	.009	.024
		Lab test	30,400	50,500	62,000	27				
	Brace	Mill rept		79,200	102,000	21	.18	.82	.010	.025
		Lab test	31,200	88,000	101,000	16				
B	Chord	Lab test	28,800	53,100	73,200	25				
	Brace	Lab test	30,100	31,700	54,200	35				
C	Chord	Mill rept		55,100	73,100	31	.23	.71	.008	.030
		Lab test	29,200	52,900	72,800	25				
	Brace	Mill rept		74,300	98,200	20	.19	.79	.010	.022
		Lab test	29,600	72,500	92,800	15				

Table 2.1 Material Properties

Description	Series		
	F	N	T-1 to T-13
Chord Dimensions, (in.)	8.61 O.D. x 0.189	8.625 O.D. x 0.202	8.625 O.D. x 0.194
σ_y of Chord Material, (ksi)	63.5	60.0	50.5
σ_u of Chord Material, (ksi)	71.5	71.0	62.0
% Elongation of Chord Material (2" Gage)	19.0	18.0	27.0
Brace Dimensions (in.)	3.77 O.D. x 0.192	3.75 O.D. x 0.195	3.75 O.D. x 0.188
σ_y of Brace Material (ksi)	63.0	63.0	88.0
σ_u of Brace Material (ksi)	79.6	79.6	101.0
% Elongation of Brace Material (2" Gage)	17.0	17.0	16.0
Area of Brace, (in^2)	2.158	2.176	2.100
Shear Area, (in^2)	2.260	2.400	2.400
$\alpha = L/a$	8.31	8.31	8.28
$\beta = c/a$ (See Fig. 2.1)	0.425	0.422	0.421
$\gamma = a/T$ (See Fig. 2.1)	22.30	20.85	21.80
$\tau = t/T$ (See Fig. 2.1)	1.020	0.965	0.968

Table 3.1 Geometrical and Material Properties of Previous T-joints (Series F & N) and Present T-joints (Series T)

Specimen	Max. Stress in Brace (ksi)	Min. Stress in Brace (ksi)	Sr in Brace (ksi)	Max. Stress in Shear Area (ksi)	Min. Stress in Shear Area (ksi)	Sr in Shear Area (ksi)	Cycles to First Crack	Cycles to Failure
F-1	7.75	1.48	5.27	7.40	1.42	5.96	9,060	11,600
F-2	5.07	0.97	4.10	4.84	0.92	3.92	40,800	67,420
F-3	5.07	0.97	4.10	4.84	0.92	3.92	57,380	76,800
N-1	8.16	1.57	6.59	7.40	1.42	5.98	4,400	12,960
N-2	8.16	1.57	6.59	7.40	1.42	5.98	6,200	14,640
N-3	8.16	1.57	6.59	7.40	1.42	5.98	8,200	20,240
N-4	8.16	1.57	6.59	7.40	1.42	5.98	3,750	7,800
N-5	5.34	1.02	4.32	4.84	0.92	3.92	39,000	75,680
N-6	5.34	1.02	4.32	4.84	0.92	3.92	54,000	99,600
N-7	5.34	1.02	4.32	4.84	0.92	3.92	27,740	46,020
N-8	6.84	1.02	5.82	5.87	0.92	4.95	5,800	16,340
N-9	6.84	1.02	5.82	5.87	0.92	4.95	3,180	13,860
N-10	6.84	1.02	5.82	5.87	0.92	4.95	3,200	8,820
N-11	6.84	1.02	5.82	5.87	0.92	4.95	2,150	11,210

Table 3.3 Fatigue test results of fourteen T-joints of previous programs (Reference 12)

Specimen	Vertical Brace*			Inclined Brace*			First Crack	Failure
	S_{max} (ksi)	S_{min} (ksi)	S_R (ksi)	S_{max} (ksi)	S_{min} (ksi)	S_R (ksi)		
K-1	3.95	1.67	2.28	-5.58	-2.39	-3.19	1,079,420	1,550,000
K-2	6.22	1.67	4.55	-8.80	-2.39	-6.41	83,000	130,330
K-3	8.50	1.67	6.83	-12.00	-2.39	-9.61	4,480	12,100
K-4	3.95	1.67	2.28	-5.58	-2.39	-3.19	1,858,670	> 2,200,000
K-5	6.22	1.67	4.55	-8.80	-2.39	-6.41	77,380	300,000
K-6	8.50	1.67	6.83	-12.00	-2.39	-9.61	27,000	65,000
K-7	3.95	1.67	2.29	-5.58	-2.39	-3.19	> 2,000,000	> 2,000,000
K-8	6.62	1.67	4.55	-8.80	-2.39	-6.41	447,500	823,080
K-9	8.50	1.67	6.83	-12.00	-2.39	-9.61	82,700	134,960

* Axial stress in brace

Table 4.2 Test Results Series - B

Series and Brace		Joint Type		
		Extended	Intersecting	Overlapping
		Kips	Kips	Kips
B	Vertical	-36	-54	-57
	Inclined	-51	-76	-81
C	Vertical	-39	-78	-94
	Inclined	-55	-110	-133

Table 4.4 Ultimate test results of K-joints

Max. Stress in Shear Area (ksi)	Min. Stress in Shear Area (ksi)	Stress Range in Shear Area (ksi)	$1/\tau$	Cycles to First Crack	Cycles to Failure
9.465	4.675	4.790	1.000	177799	247300
9.465	4.675	4.790	1.000	157000	229400
3.709	-.041	3.750	1.000	243002	369600
5.143	.813	4.330	1.000	45900	107900
4.271	.661	3.610	1.000	163799	291500
1.915	-1.915	3.830	1.000	93300	312800
3.745	-3.745	7.490	1.000	12400	23500
6.889	1.119	5.770	1.000	21800	34100
6.889	1.119	5.770	1.000	21900	39100
1.915	-1.915	3.830	1.000	184200	412800
2.891	0.000	2.891	1.000		718040
3.745	-3.745	7.490	1.000	5000	13600
4.795	-4.795	9.590	1.000	3500	3600
2.860	-2.860	5.720	.833	72000	481900
3.270	-3.270	6.540	.833	25500	68600
3.270	-3.270	6.540	.833	24000	36200
3.270	-3.270	6.540	.833	23500	66400
2.860	-2.860	5.720	.833	44300	103600
2.860	-2.860	5.720	.833	49000	101100
2.465	-2.465	4.930	.833	121199	240600
2.465	-2.465	4.930	.833	88499	242600
2.860	-2.860	5.720	.833	32200	137000
2.465	-2.465	4.930	.833	263003	883600
2.880	-2.880	5.760	.918	386999	657800
2.555	-2.555	5.110	.918	215998	531500
2.140	-2.140	4.280	.918	2500979	4104000
2.880	-2.880	5.760	.918	1672014	1963620
2.880	-2.880	5.760	.918	2823969	4324350
2.855	-2.855	5.710	1.674	58600	137200
3.055	-3.055	6.110	1.674	234002	293000
3.055	-3.055	6.110	1.674	477002	502400
2.855	-2.855	5.710	1.674	477002	568800
2.855	-2.855	5.710	1.674	764997	799800
2.495	-2.495	4.990	1.674	1517015	1809300
2.495	-2.495	4.990	1.674	3152028	3210900
3.055	-3.055	6.110	1.674	230399	257800
2.855	-2.855	5.710	1.674	1061011	1060900
2.855	-2.855	5.710	1.674	332997	480600
1.551	0.000	1.551	1.000		1062000
3.055	-3.055	6.110	1.674	377998	433800
2.855	-2.855	5.710	1.674	169001	239600
2.495	-2.495	4.990	1.674	142200	271800
2.495	-2.495	4.990	1.674	1160994	1414700

Table 5.1 Small T-joints (Continued)

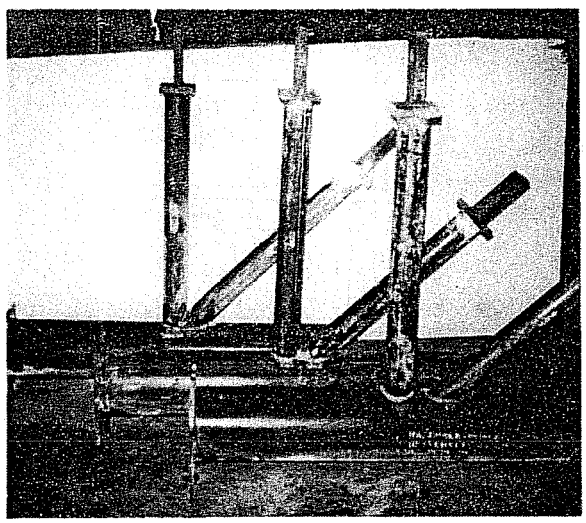

Fig. 1.1 The three different types of K-joints in series B

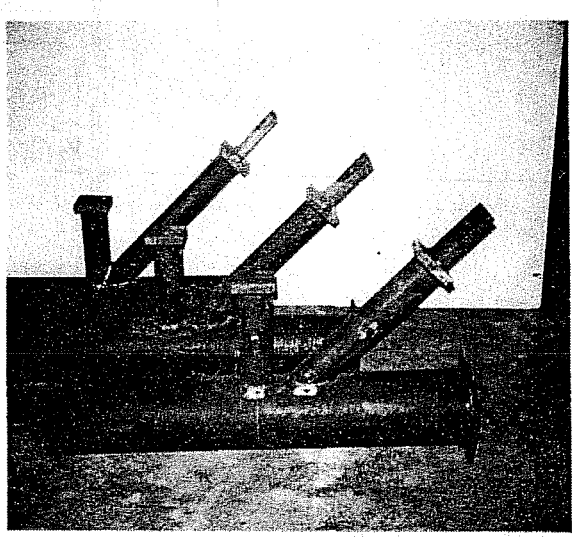

Fig. 1.2 The three different types of K-joints in series C

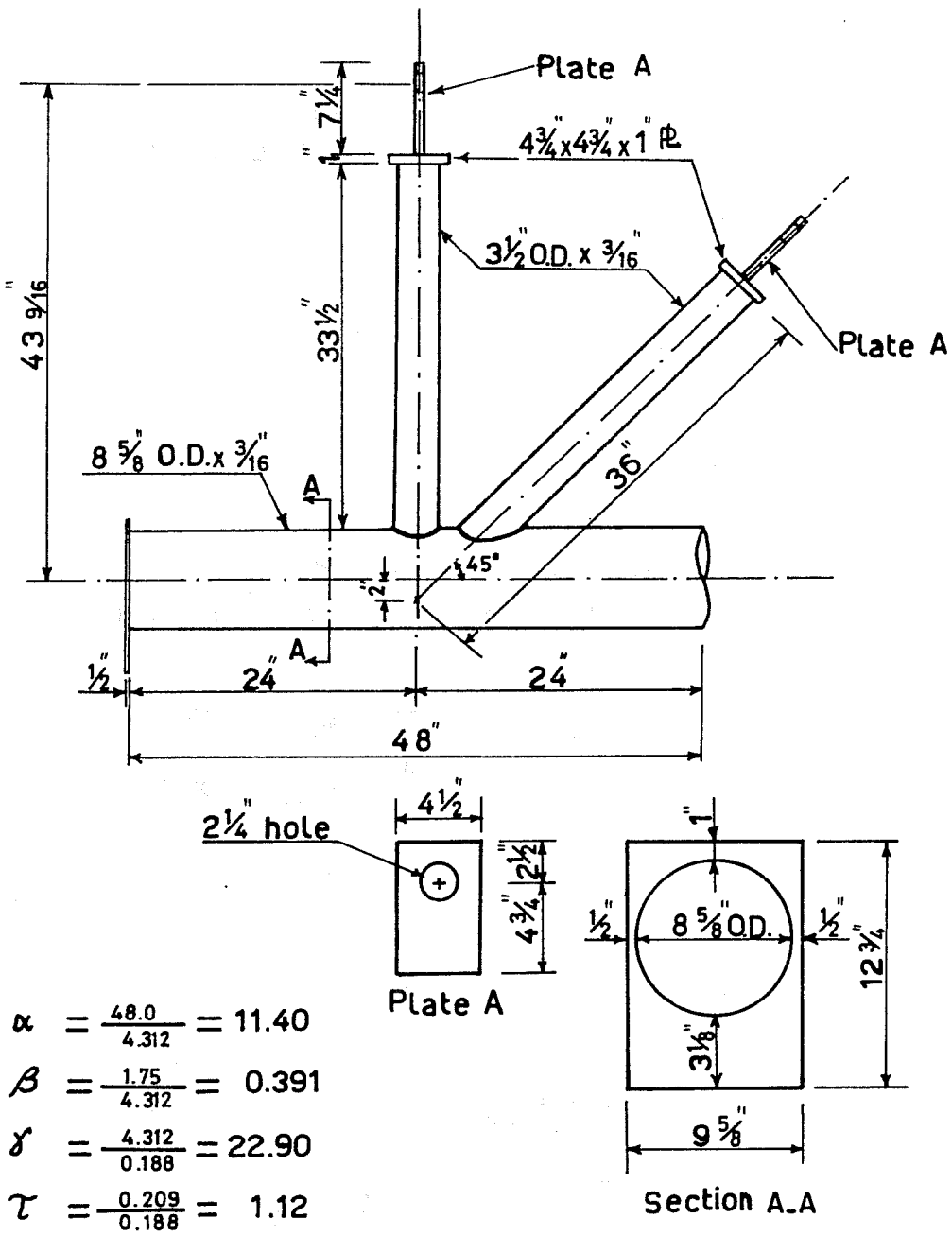

$$\alpha = \frac{48.0}{4.312} = 11.40$$

$$\beta = \frac{1.75}{4.312} = 0.391$$

$$\gamma = \frac{4.312}{0.188} = 22.90$$

$$\tau = \frac{0.209}{0.188} = 1.12$$

(a) Extended case (K-1,2 &3)

Fig.2.2 Series B specimens (Continued)

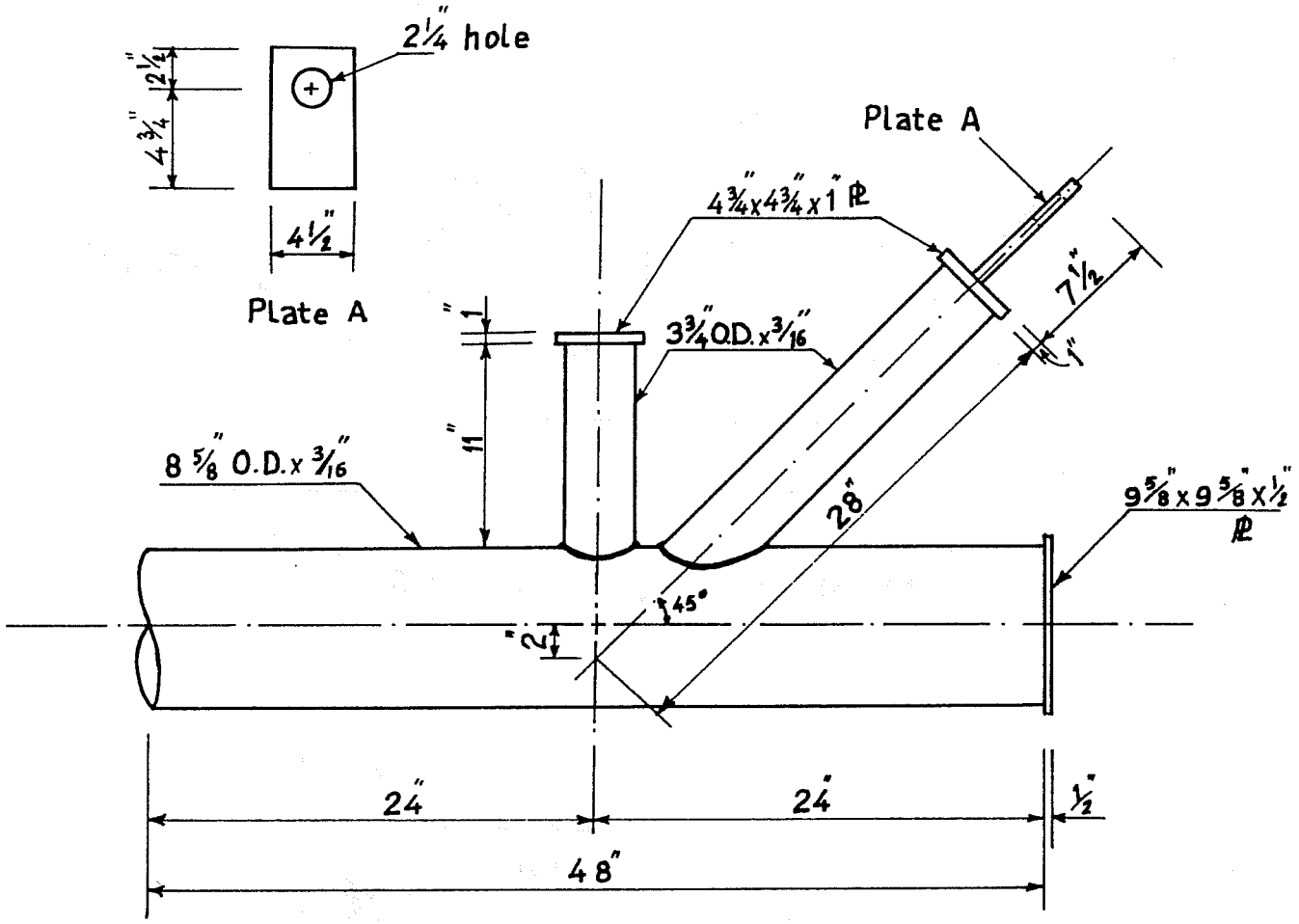

$$\alpha = \frac{48.0}{4.312} = 11.40$$

$$\beta = \frac{1.815}{4.312} = 0.421$$

$$\gamma = \frac{4.312}{0.183} = 23.56$$

$$\tau = \frac{0.190}{0.183} = 1.04$$

(a) Extended case (K_10,11&12)

Fig.2.3 Series C specimens (Continued)

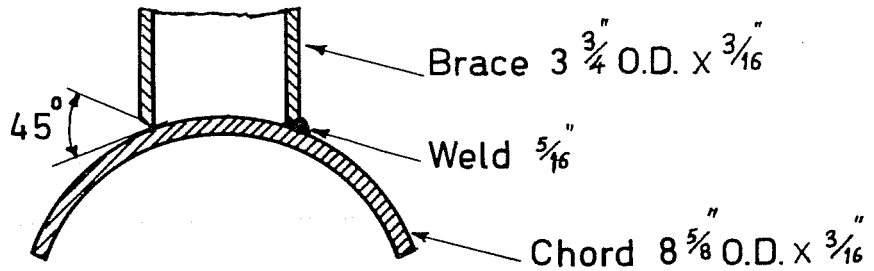

Fig. 2.4 Typical weld of a joint

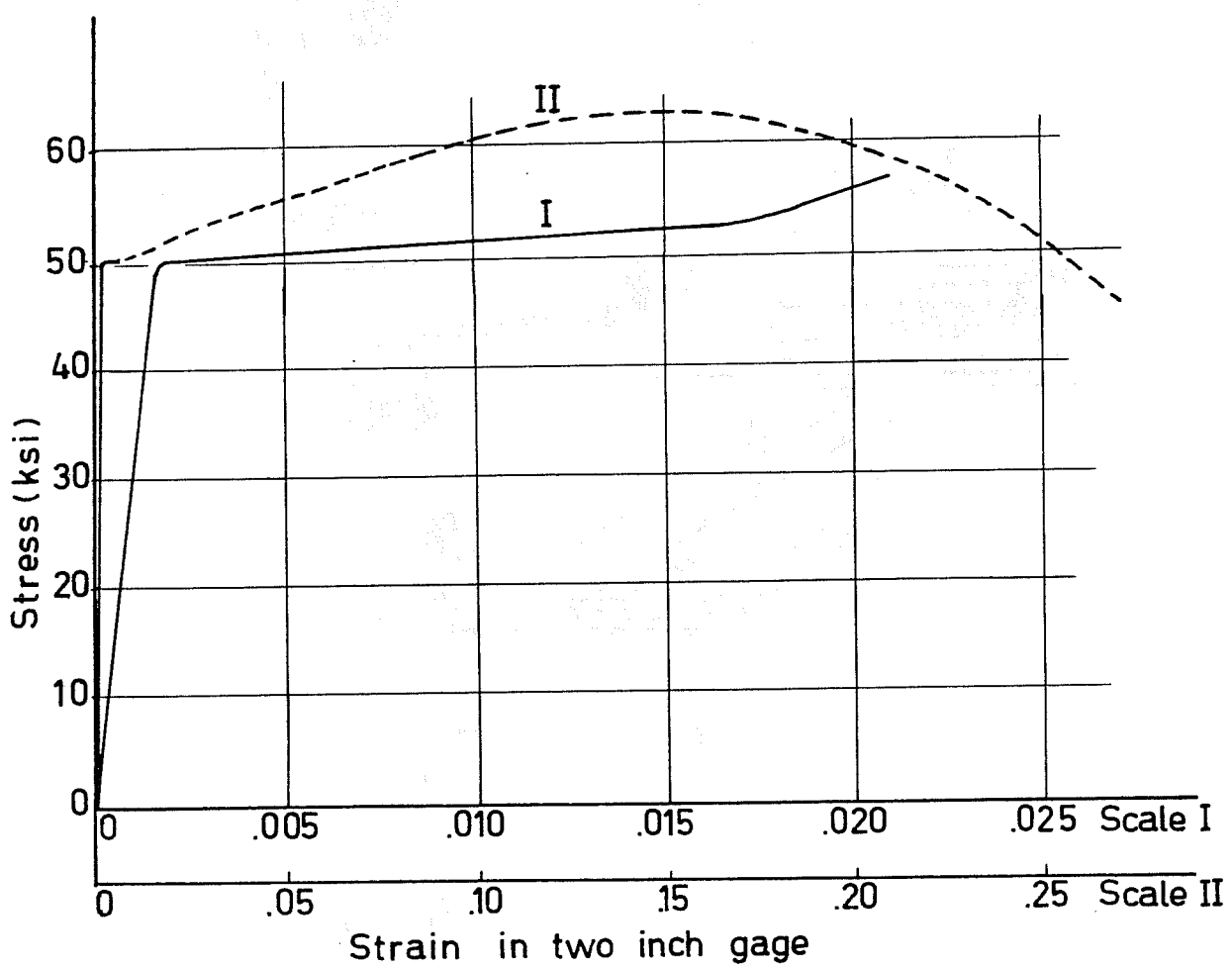

Fig. 2.5 Typical stress_strain curve (chord in T-joints)

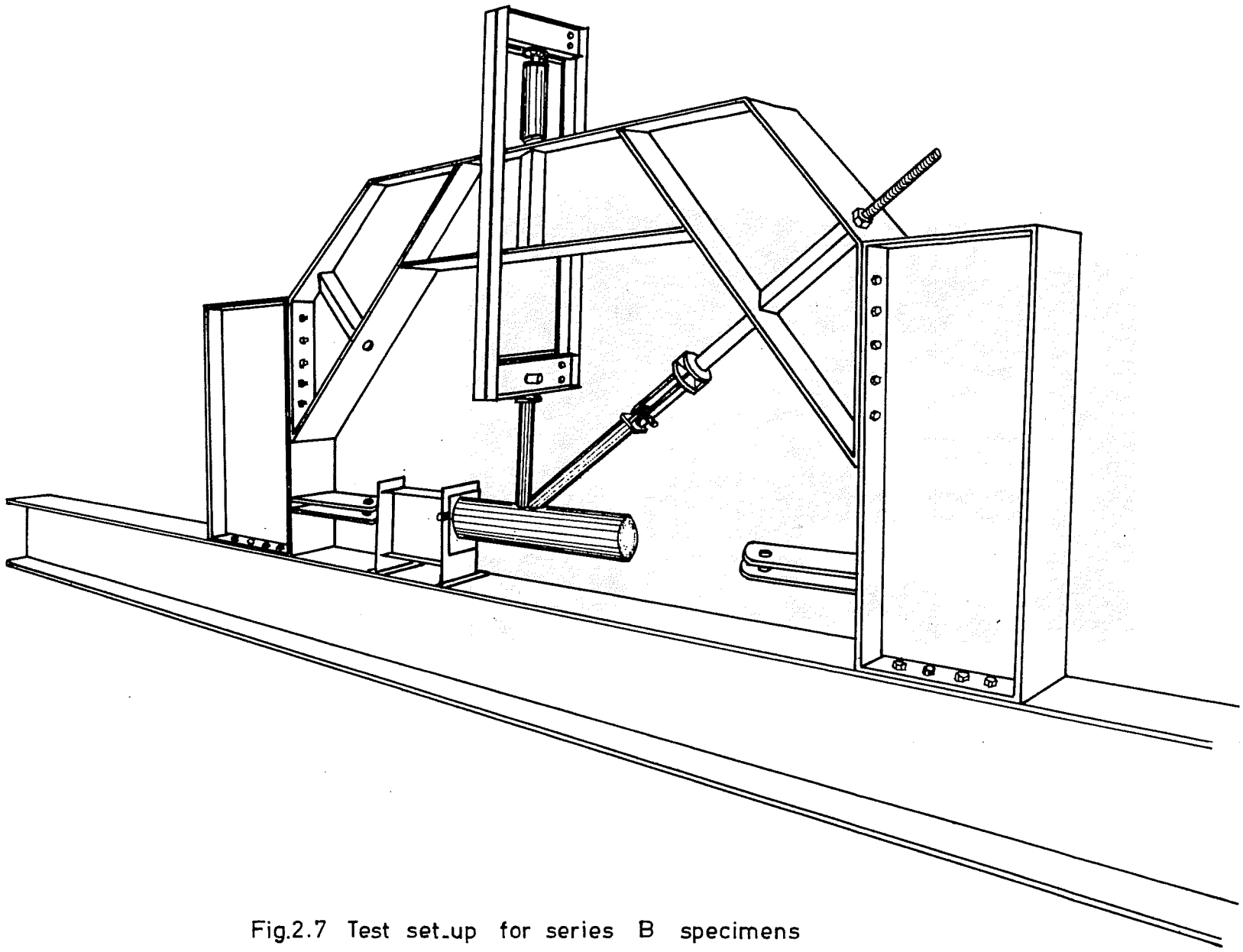

Fig.2.7 Test set_up for series B specimens

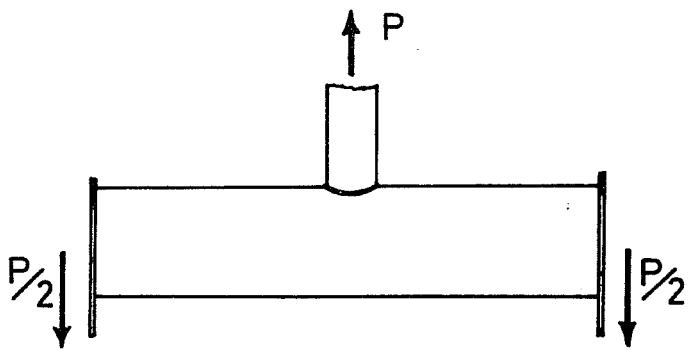

Fig.3.1 Load application in T_joints

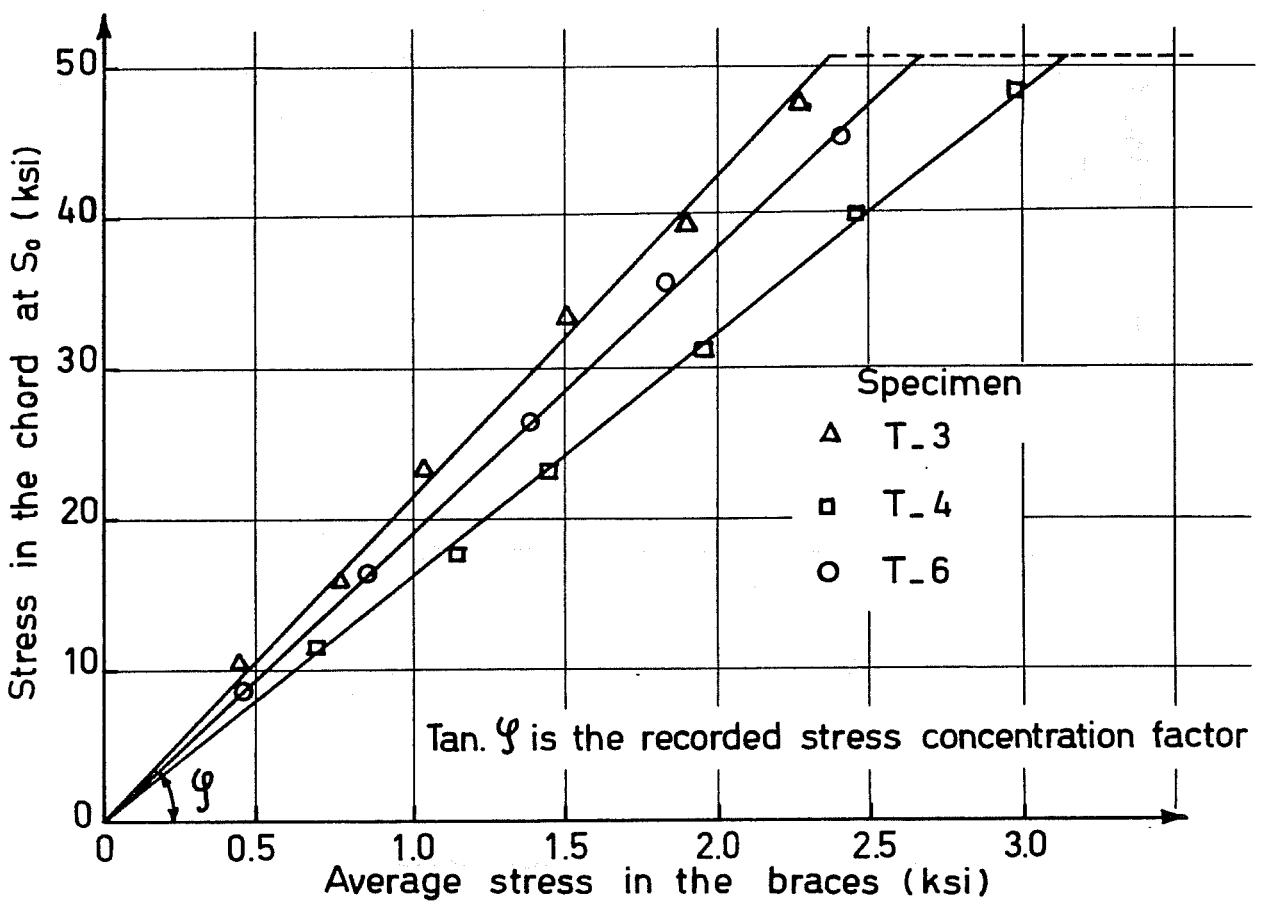

Fig. 3.2 Measured stresses at S_o

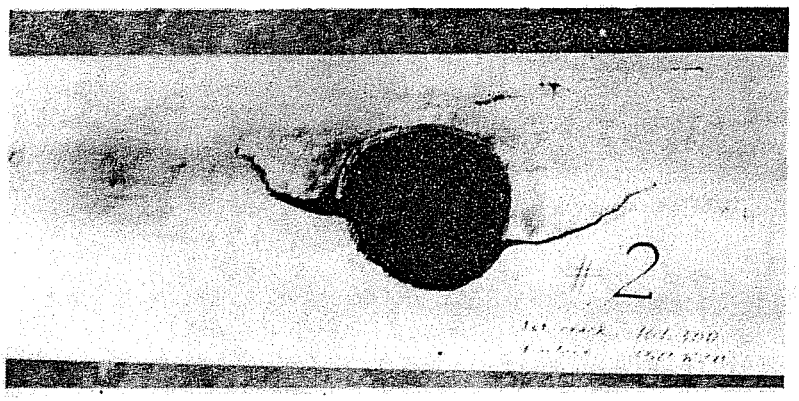

Fig. 3.4 Fatigue failure of T-2 (cracked on one side)

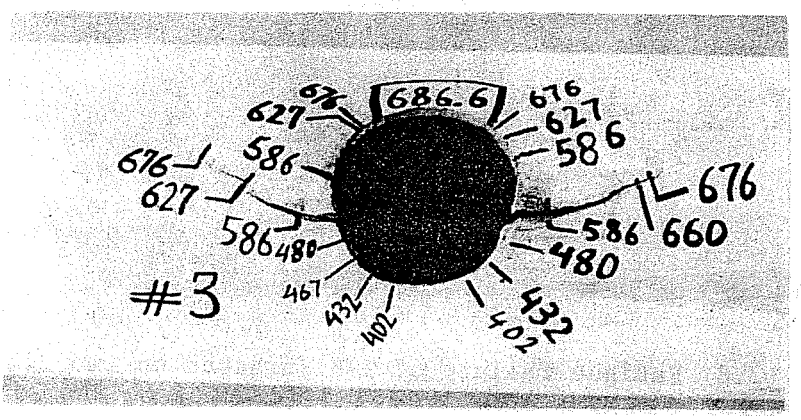

Fig. 3.5 Fatigue failure of T-3 (cracked on one side)

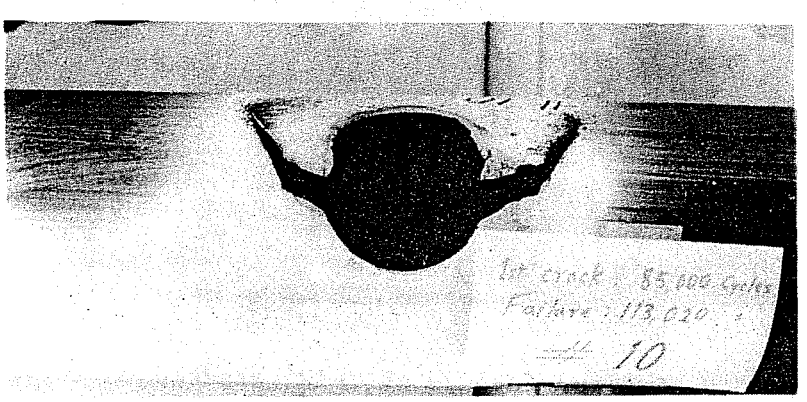

Fig. 3.6 Fatigue failure of T-10 (cracked on one side)

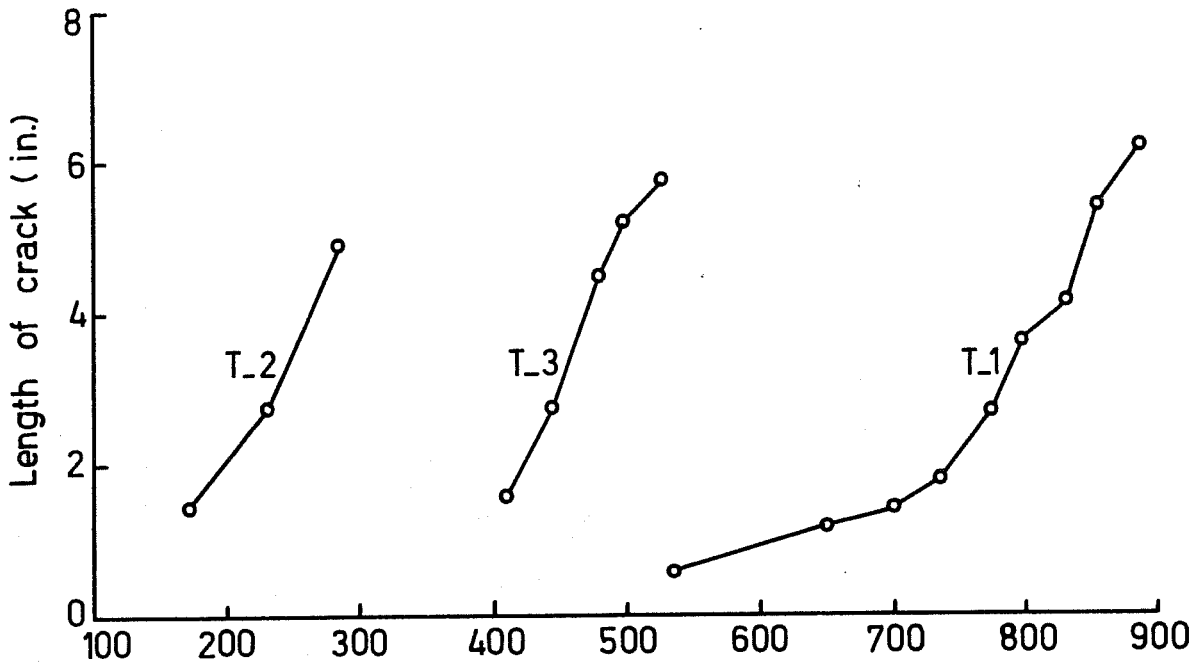

(a)

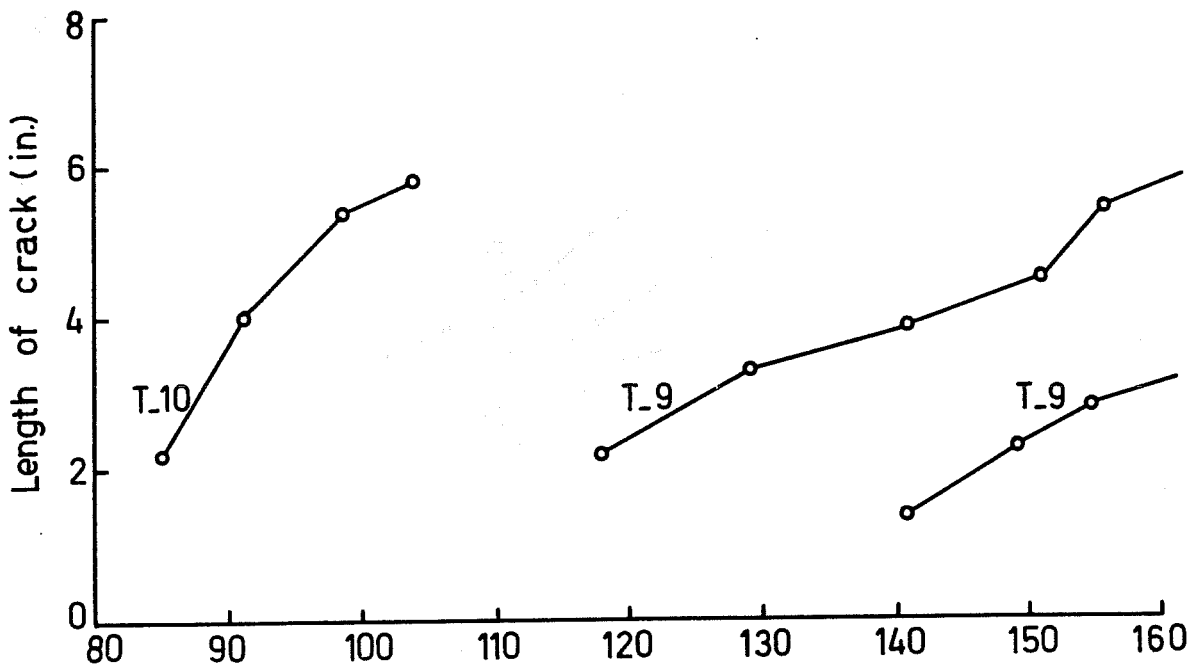

(b)

Fig.3.10 Crack propagation in T_joints (Continued)

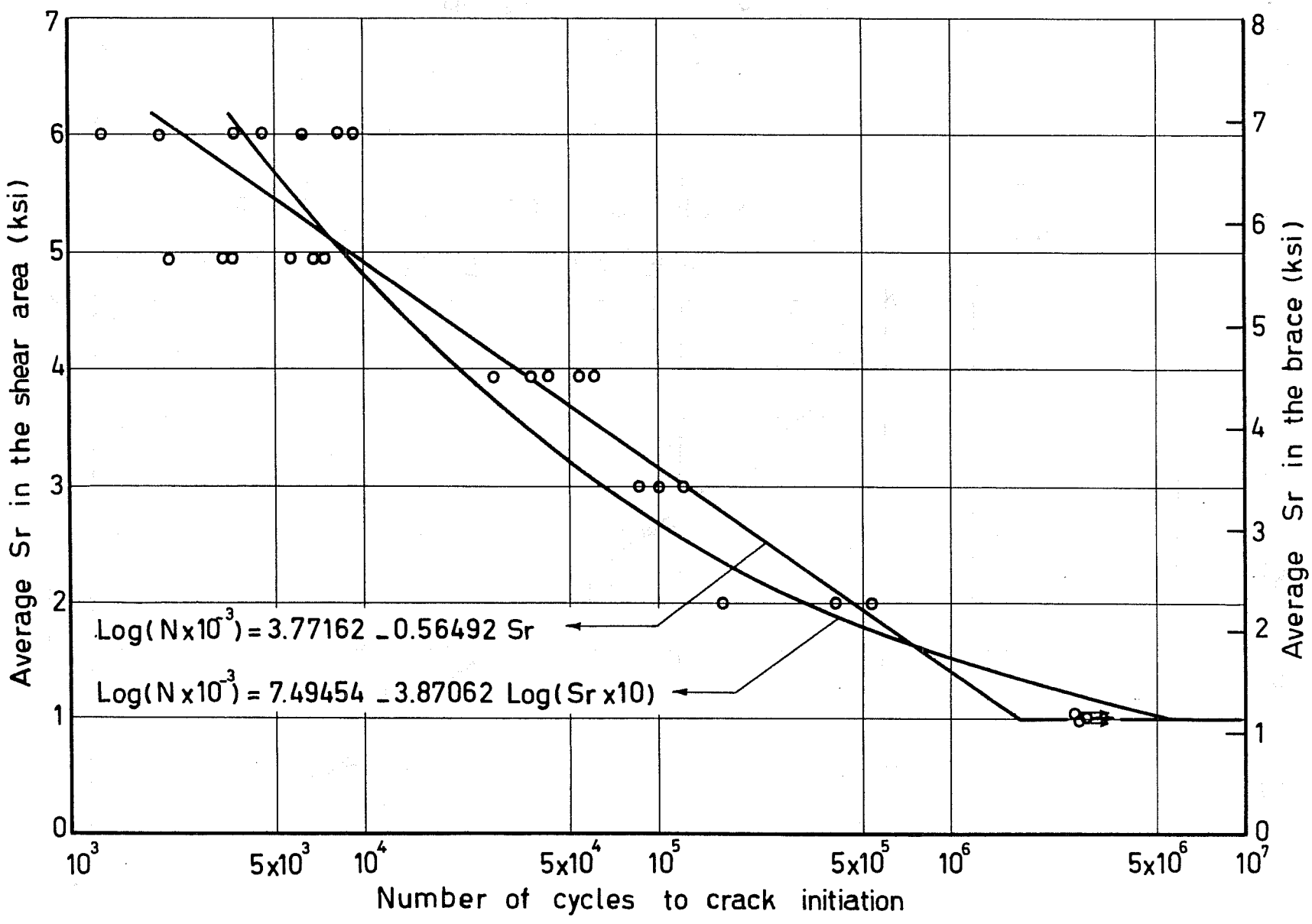

Fig. 3.11 S-N curve for crack initiation in T-joints

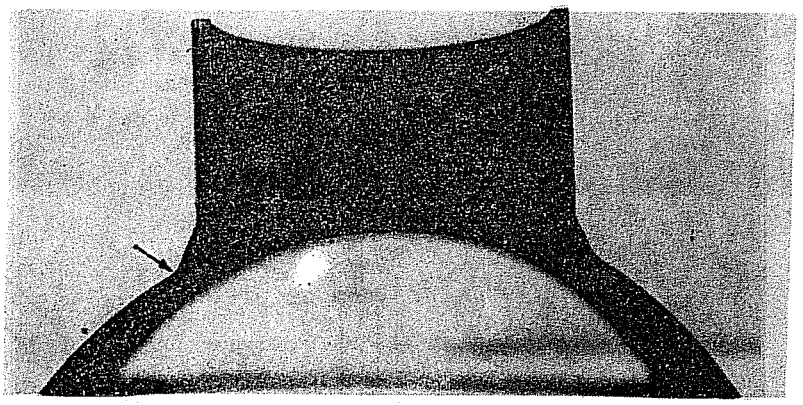

Fig. 3.13 Section in T-13 showing the weld

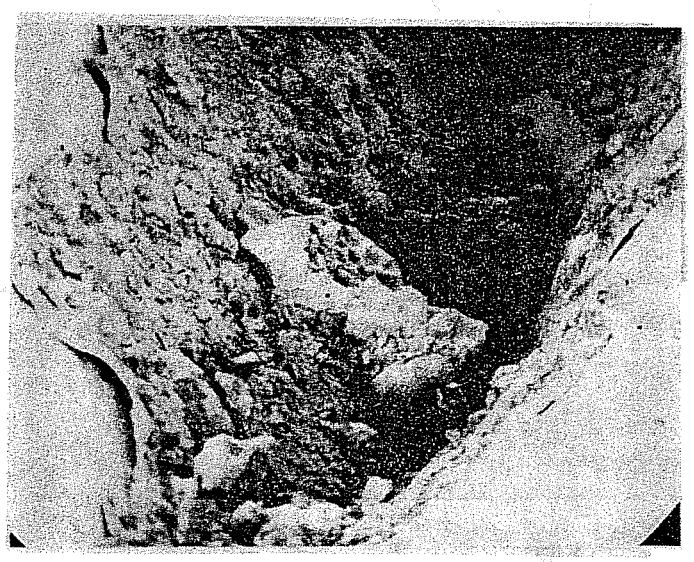

Fig. 3.14 Notch at the toe of the weld

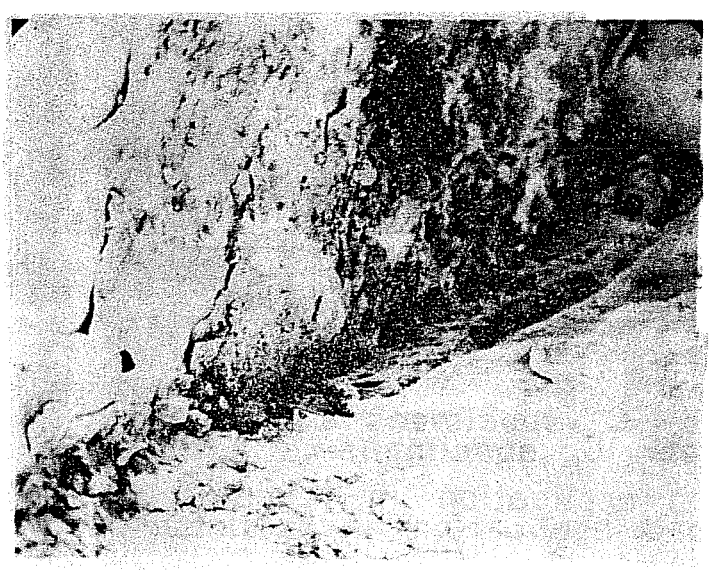

Fig. 3.15 Electron microscope photograph of the separating line between weld and chord materials

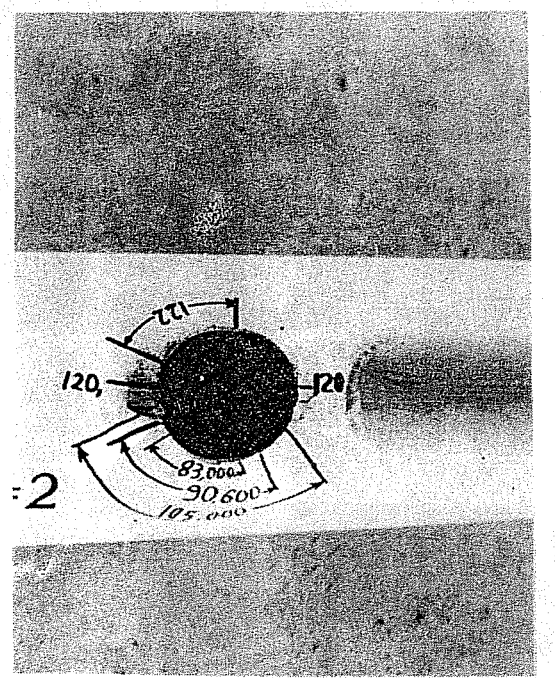

Fig. 4.2 Fatigue failure of K-2

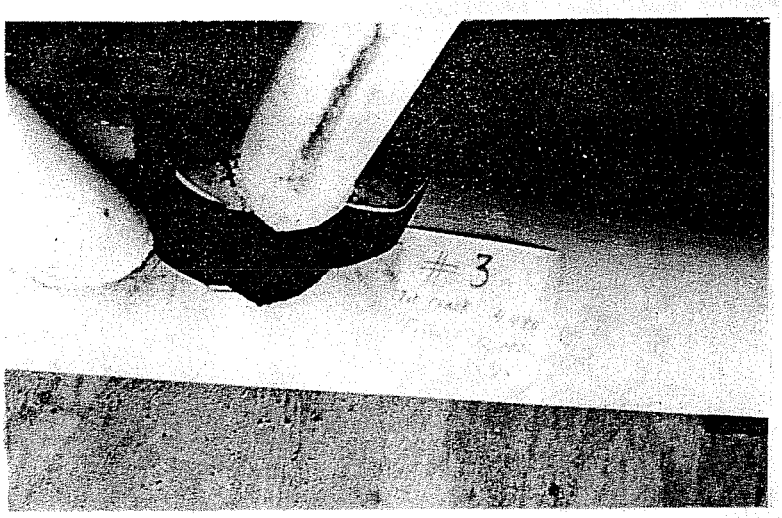

Fig. 4.3 Fatigue failure of K-3

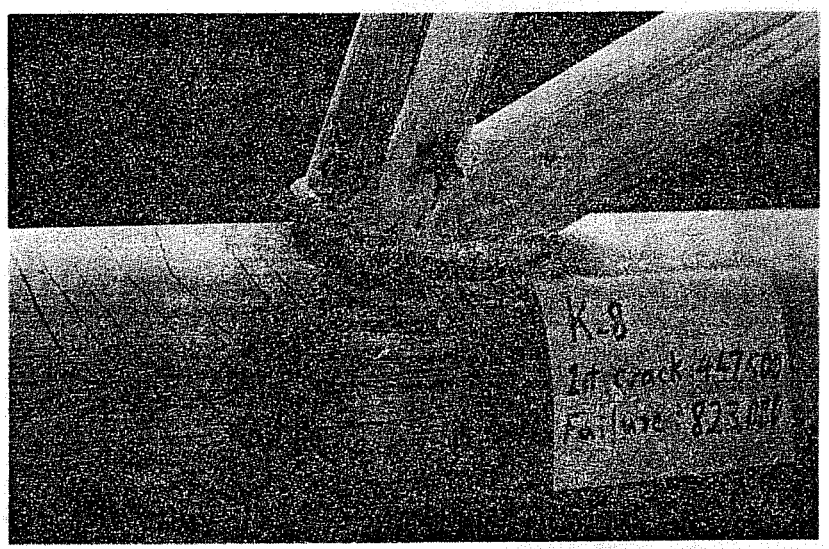

Fig. 4.7 Fatigue failure of K-8

Fig. 4.8 Fatigue failure of K-9

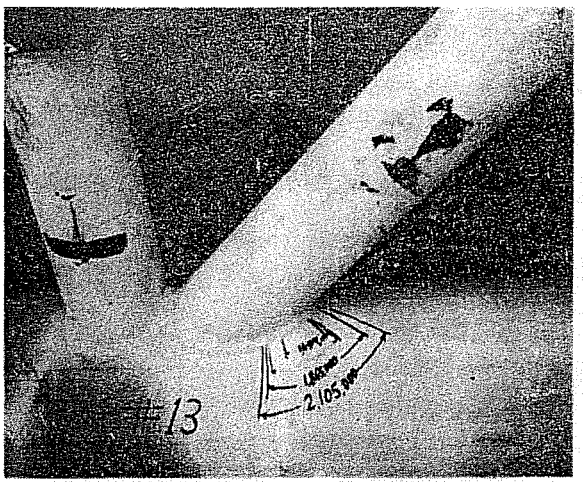

Fig. 4.12 Fatigue failure of K-13

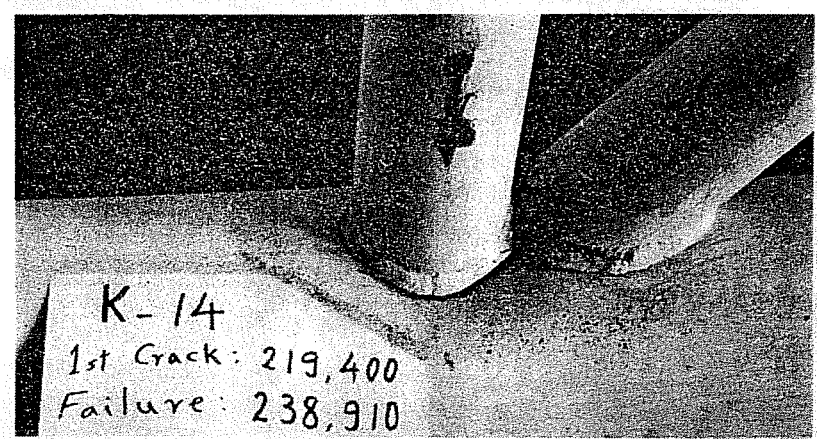

Fig. 4.13 Fatigue failure of K-14

Fig. 4.14 Fatigue failure of K-15

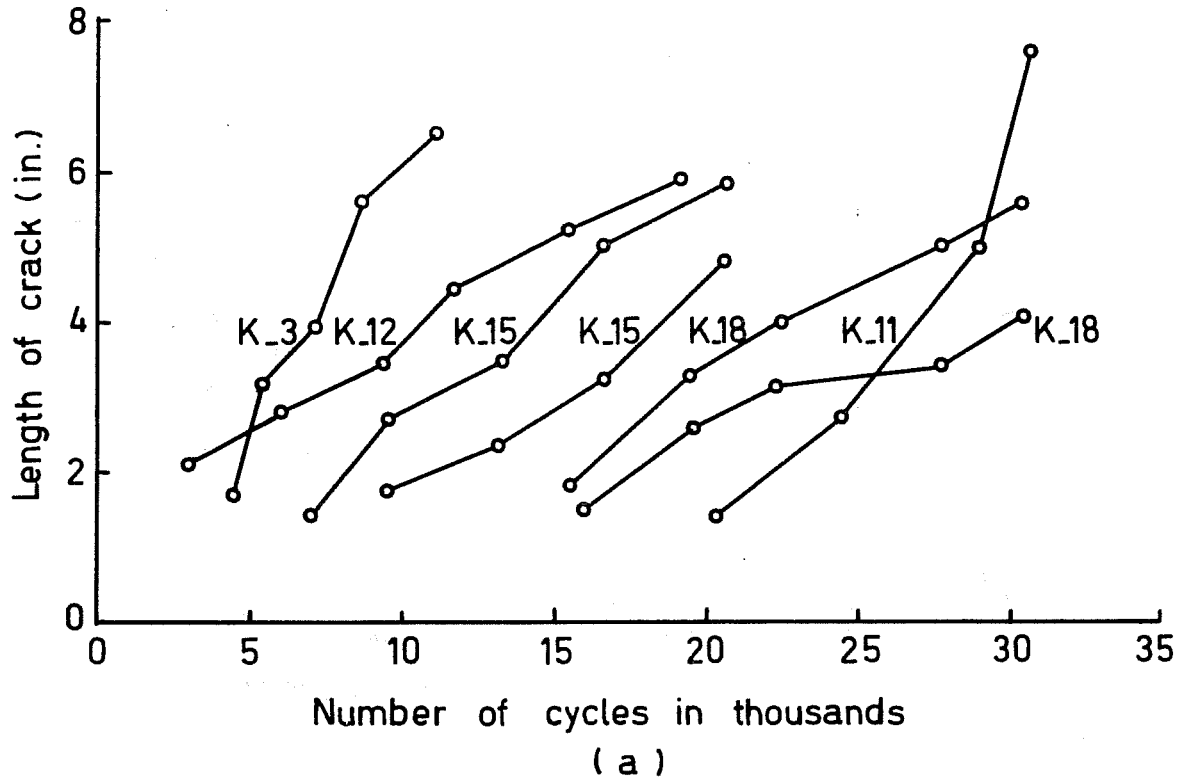

(a)

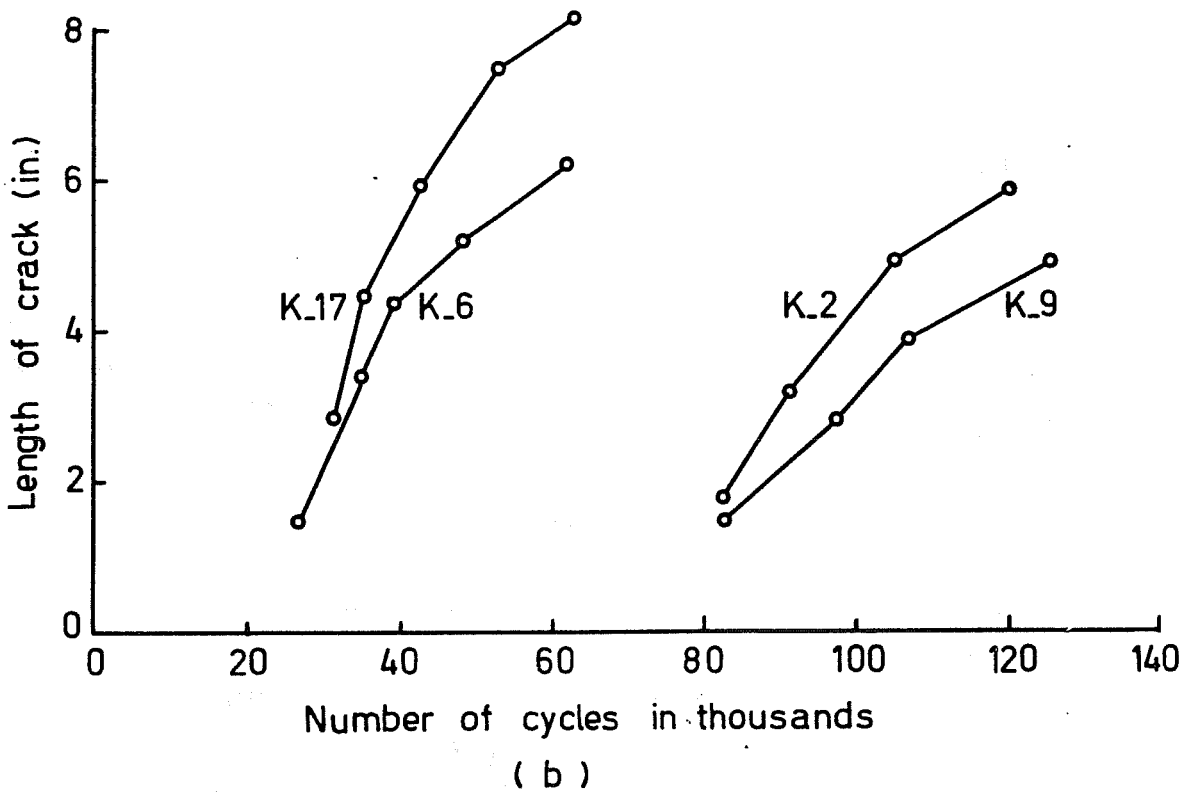

(b)

Fig.4.17 Crack propagation in K_joints (Continued)

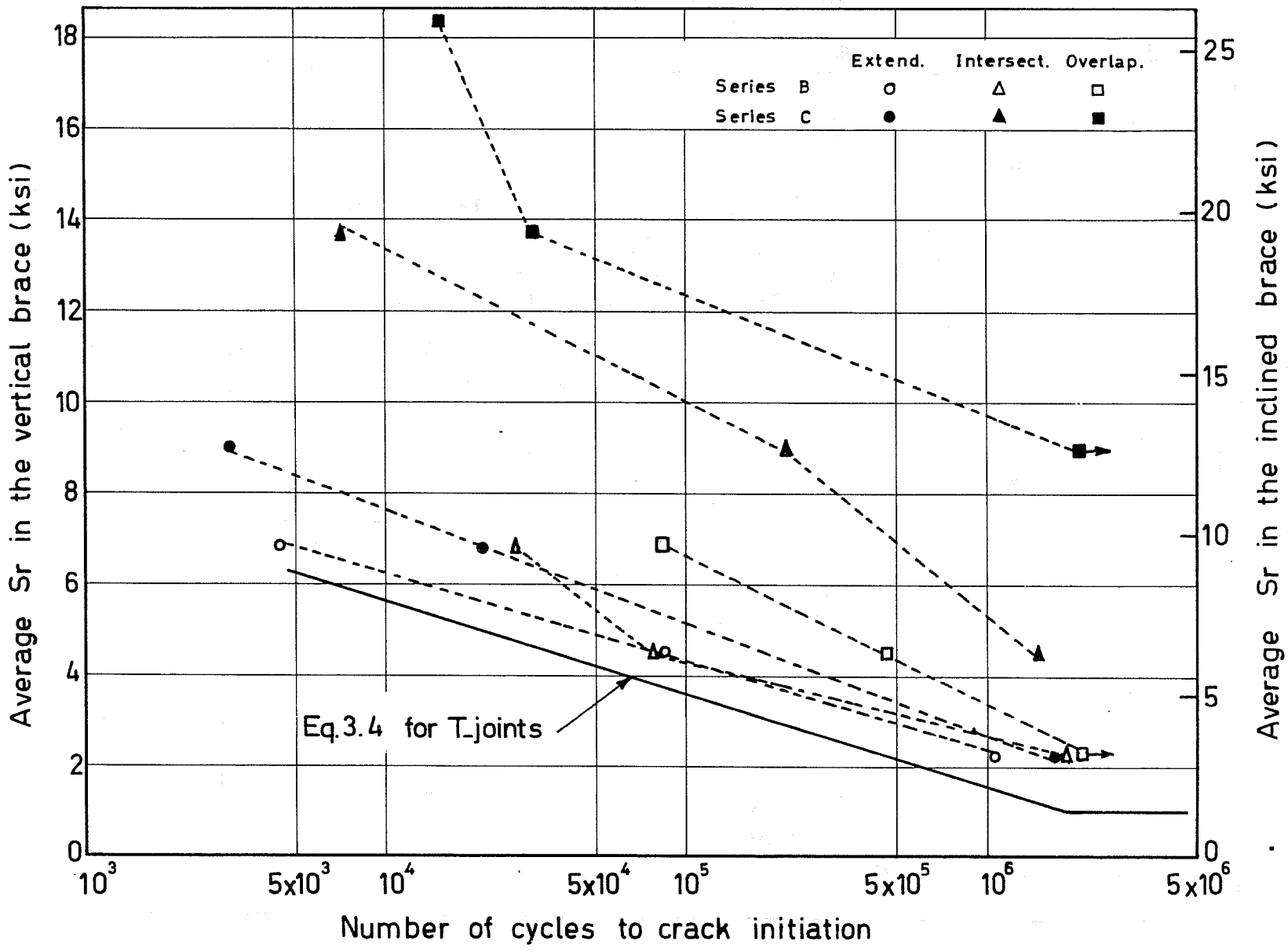

Fig.4.18 S_N curves for crack initiation in K_joints

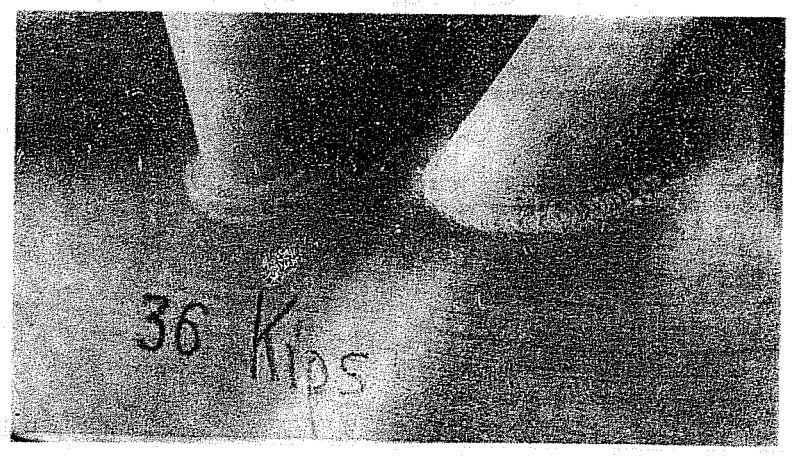

Fig. 4.20 Static load failure in K-joint (series B) with extended braces

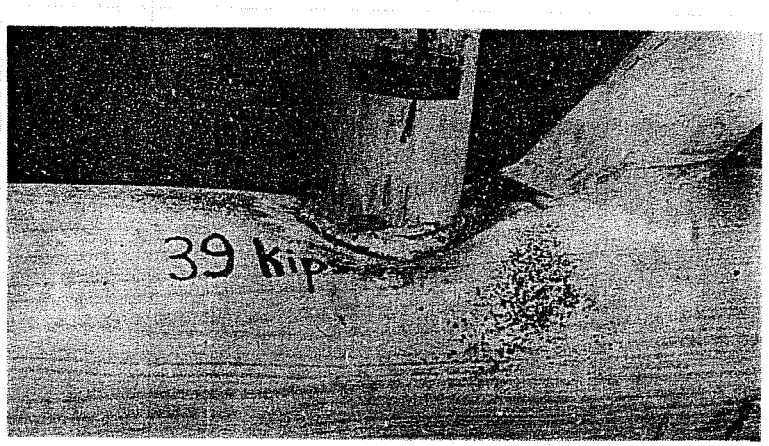

Fig. 4.21 Static load failure in K-joint (series C) with extended braces

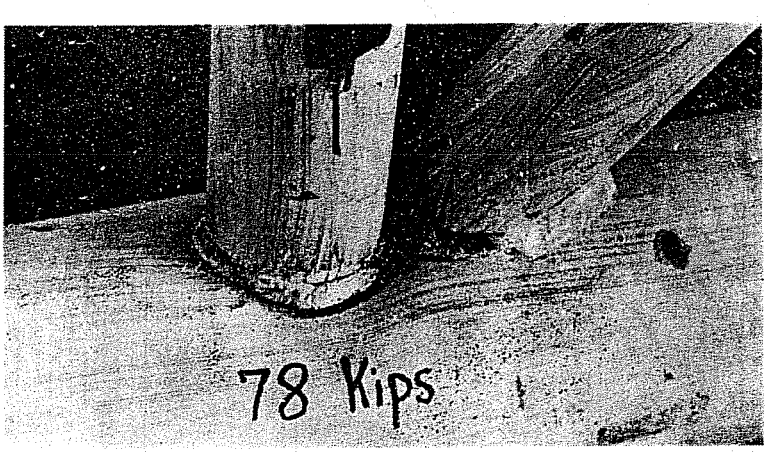

Fig. 4.22 Static load failure in K-joint (series C) with intersecting braces

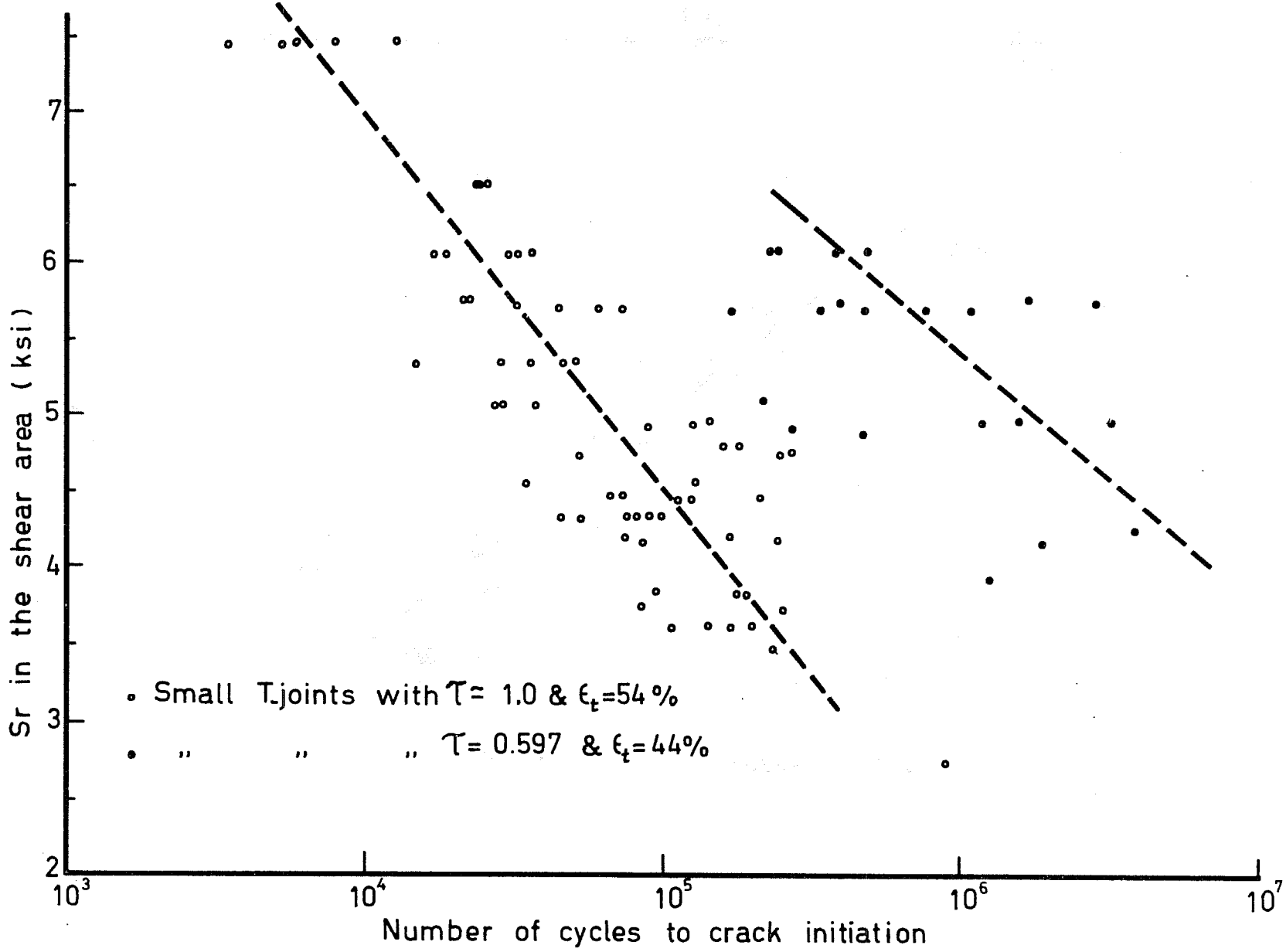

Fig.5.2 S-N curves for small T-joints

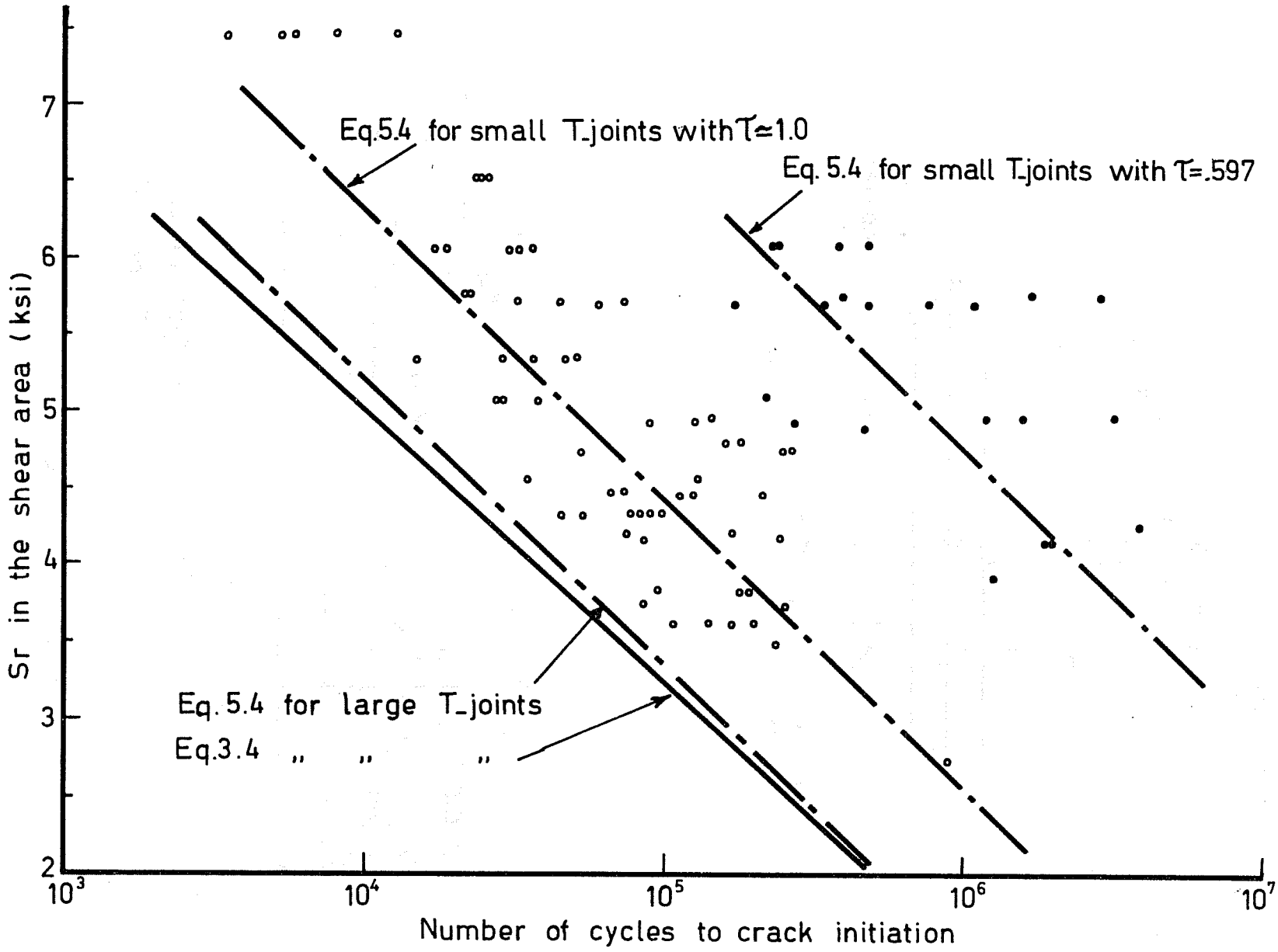

Fig.5.4 Eq.5.4 and S-N curves for large and small T-joints

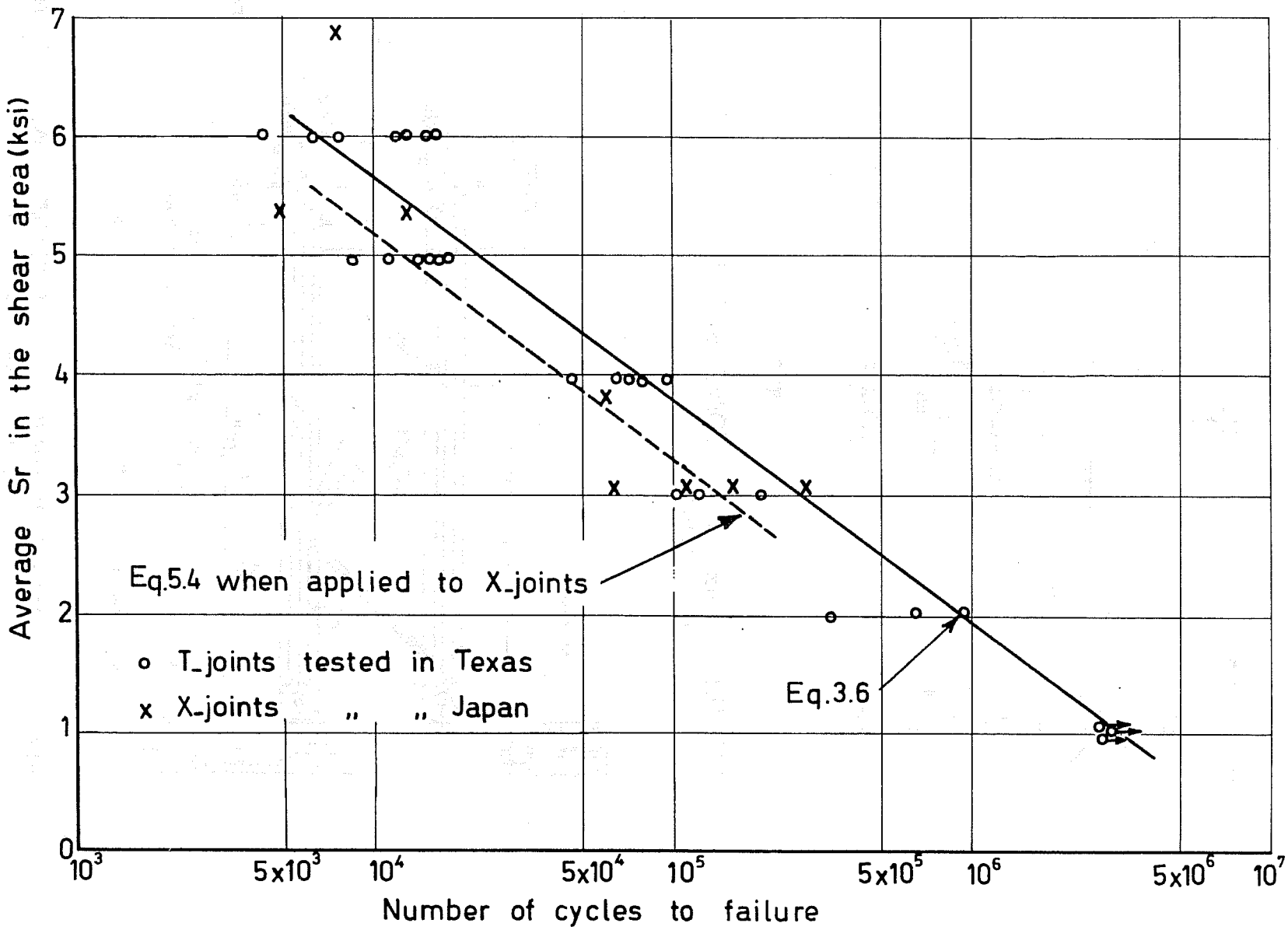

Fig.5.7 S_N relationship of T_ and X_joints

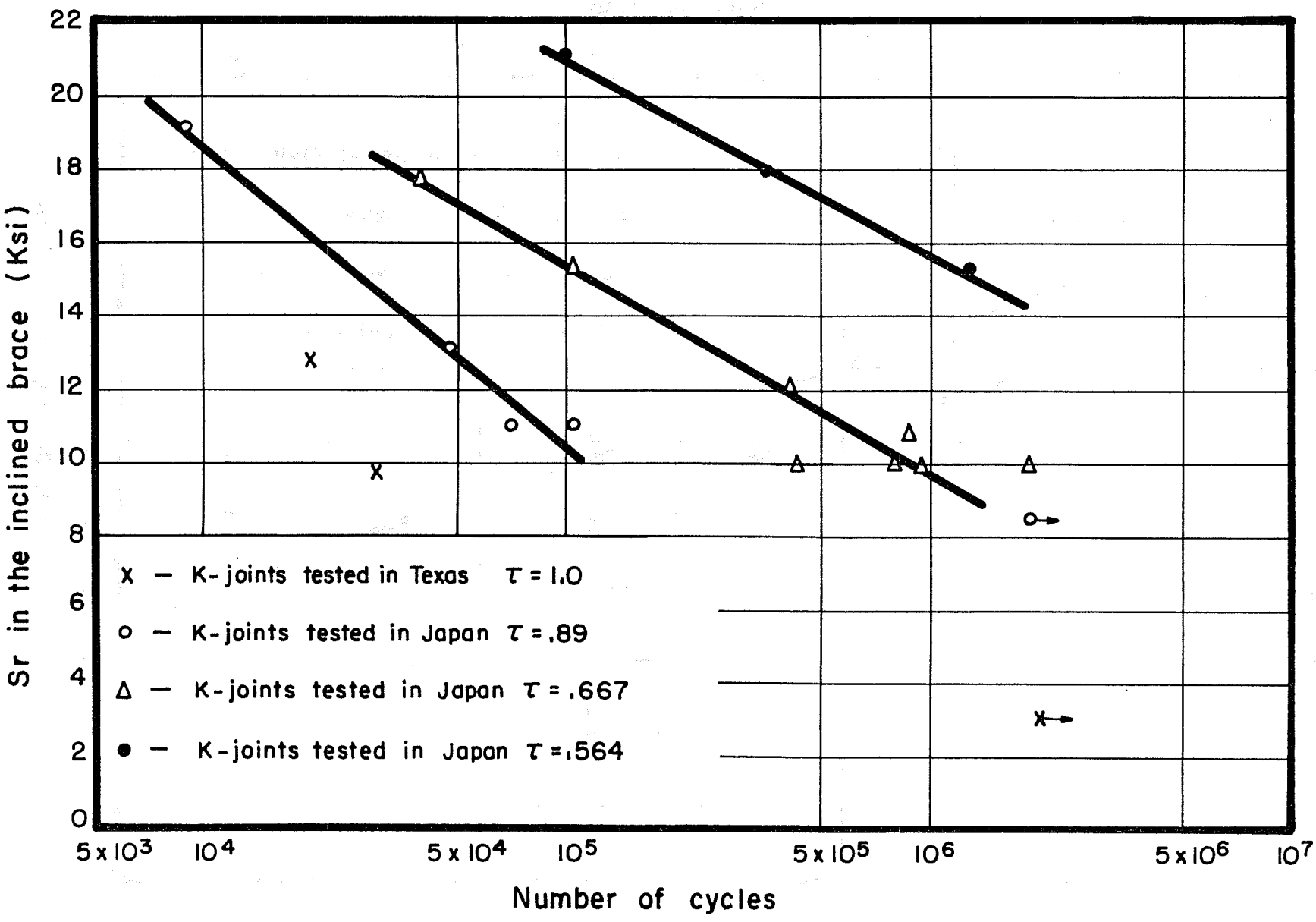

FIG. 5.9 S-N RELATIONSHIP FOR K-JOINTS TESTED IN JAPAN (I)

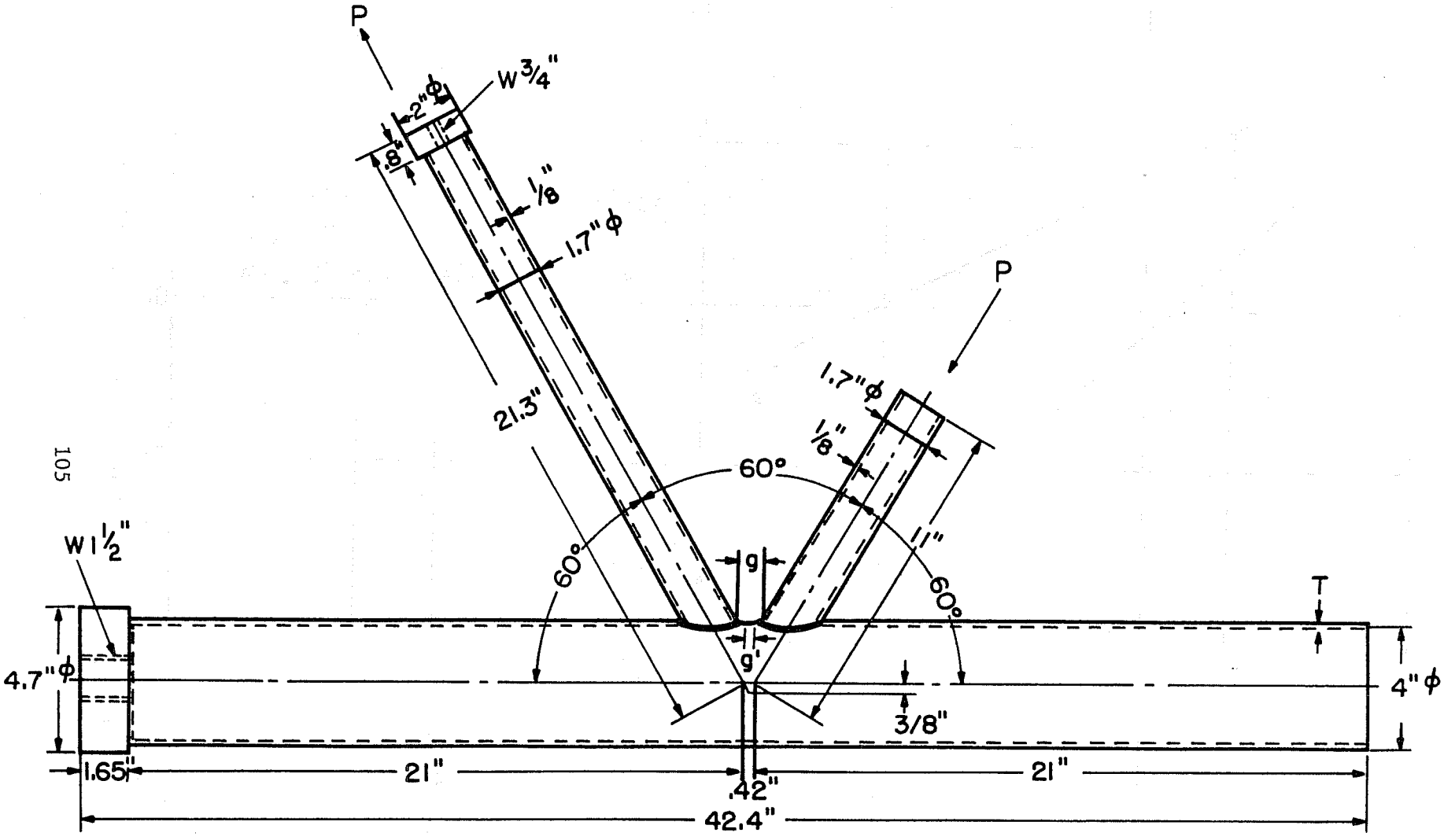

FIG. 5.11 K-JOINT SPECIMEN TESTED IN JAPAN (II).

APPENDIX A

NOMENCLATURE AND COORDINATE SYSTEM

a	mean chord radius.
c	mean brace radius.
L	length of chord.
T	chord thickness.
t	brace thickness.
S	circumferential coordinate axis at the vertical brace.
S'	circumferential coordinate axis at the inclined brace.
S_o	point where the S axis intersects the weld toe (Vertical brace).
S'_o	point where the S' axis intersects the weld toe (Inclined brace).
X	longitudinal coordinate axis for vertical brace.
X_o	point where the X axis intersects the weld toe (Vertical brace).
X'_o	point where the X axis intersects the weld toe (Inclined brace).
α	= L/a, the chord length parameter.
β	= c/a, the brace radius parameter.
γ	= a/T, the chord thickness parameter.
τ	= t/T, the brace thickness parameter.
θ	angle between the brace and chord axes.
R	ratio of minimum load over maximum load in fatigue.
σ_y	yield stress.
σ_u	ultimate stress.
σ_{ss}	the stress along the S axis in circumferential direction.

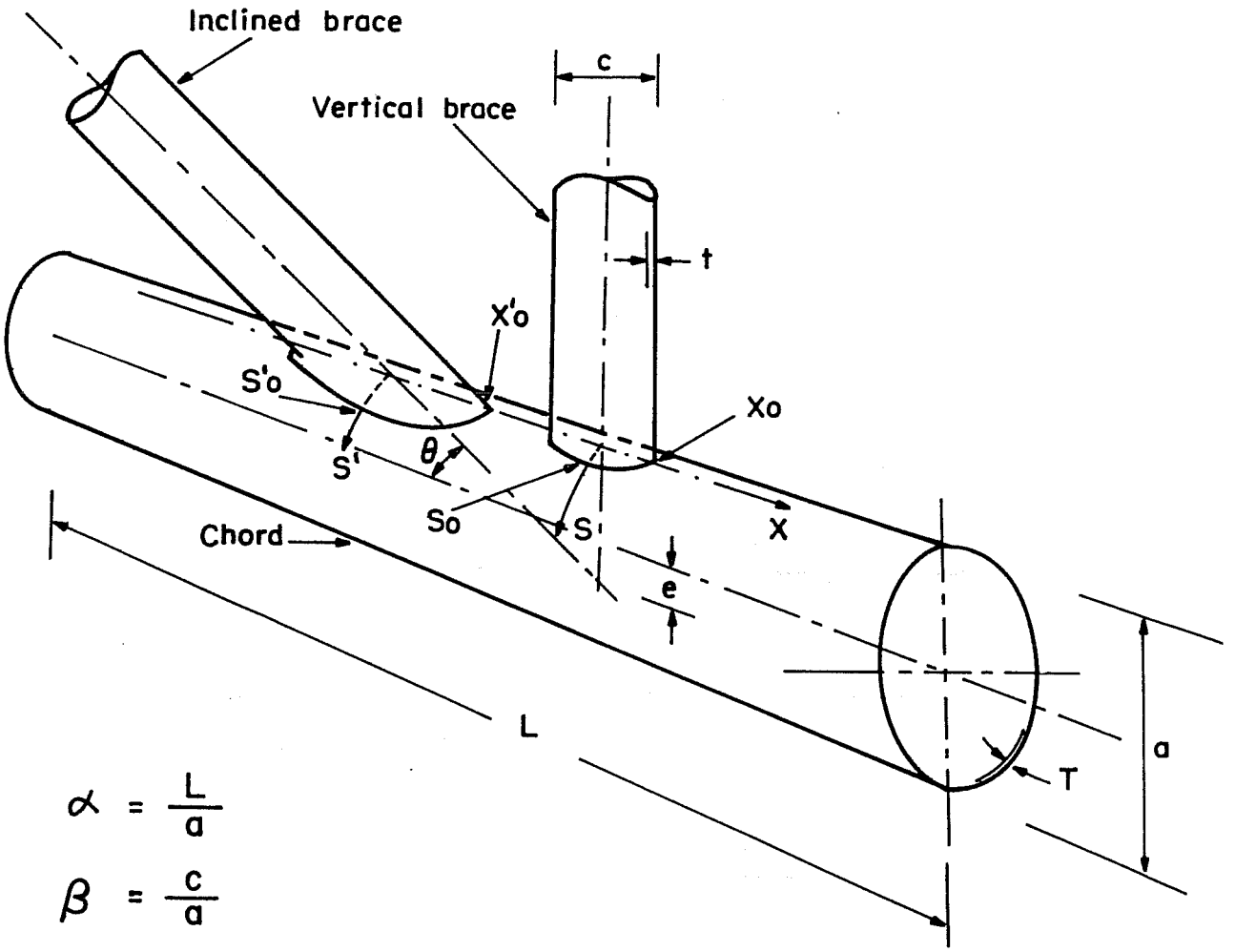

$$\alpha = \frac{L}{a}$$

$$\beta = \frac{c}{a}$$

$$\gamma = \frac{a}{T}$$

$$\tau = \frac{t}{T}$$

FIG. A.I COORDINATE SYSTEM USED FOR T- AND K-JOINT SPECIMENS.

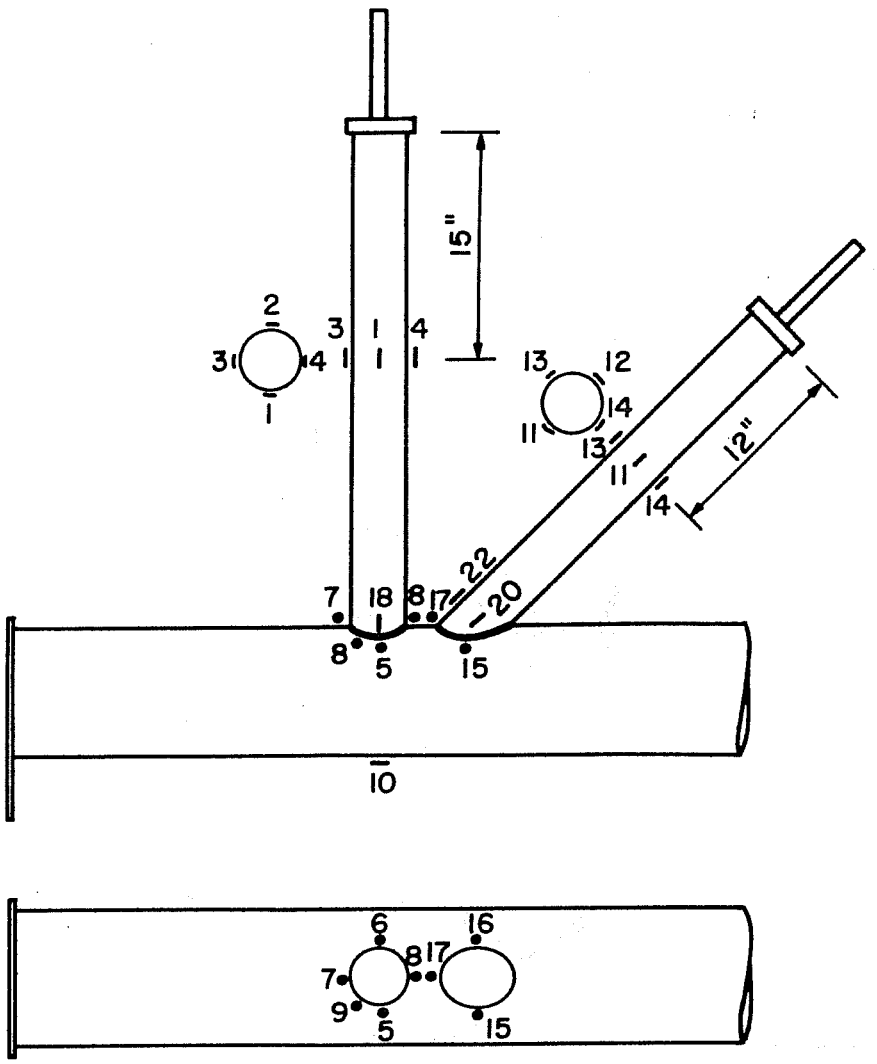

Rosette gages were installed in locations 5, 6, 7, 8, 9, 15, 16 and 17.

FIG. B.2 STRAIN GAGE LOCATIONS IN K-1, 2 & 3.

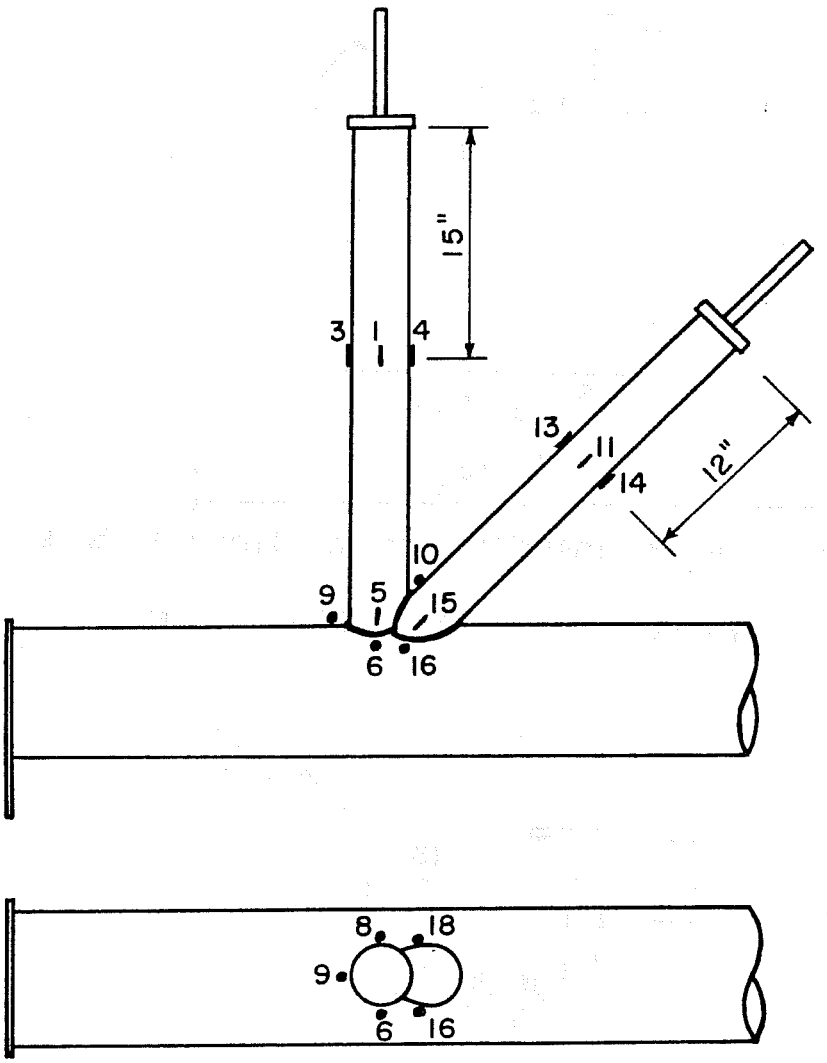

Rosette gages were installed at locations 6, 8, 9, 10, 16 and 18.

FIG. B.4 STRAIN GAGE LOCATIONS IN K.7, 8 & 9.

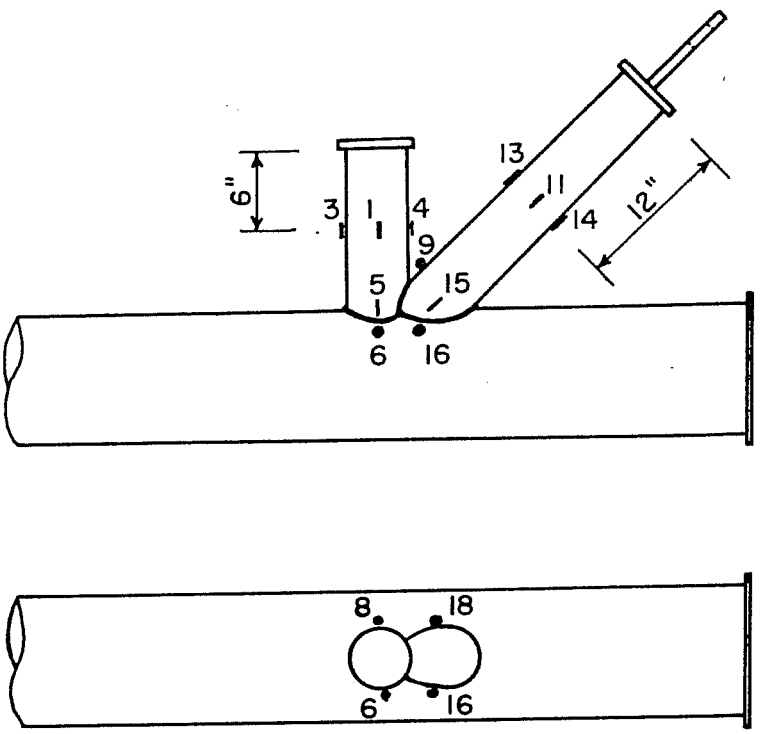

Rosette gages were installed at locations 6,8,9, 16 & 18.

FIG. B.7 STRAIN GAGE LOCATIONS IN K-16, 17 & 18.